Optical imaging of intrinsic signals during ocular dominance plasticity
in a conditional aggrecan knockout mice

Master thesis in Molecular Bioscience

Main field in physiology and neurobiology

Rune Alexander Lanton

60 credits

Program for Physiology and Neurobiology

Department of Biosciences

The Faculty of Mathematics and Natural Sciences

UNIVERSITY OF OSLO

2015

2015

Optical imaging of intrinsic signals during ocular dominance plasticity in a conditional aggrecan knockout mice.

Rune Alexander Lanton

http://www.duo.uio.no/

Print: Reprosentralen, University of Oslo

Abstract

The nervous system has large capacity to change based on experience and adapt to changes in the environment. However, the level of plasticity is not constant, varying between brain regions and during the development of the animal. These changes imply the existence of mechanisms regulating the level of neuronal plasticity. Recent studies have pointed towards extracellular matrix structures called the perineuronal nets (PNNs) to be important. Experimental disintegration of the PNNs has been shown to increase plasticity in the central nervous system. However, PNNs consist of complex proteoglycan molecules and the functional role of the different components remains unclear. The lectican called aggrecan is a large proteoglycan that has been suggested to have an important role for functional PNNs. However, aggrecan is a critical component of cartilage, and mice deficit in aggrecan will die at birth. This has made it impossible to carry out *in-vivo* studies in constitutive aggrecan knockout animals.

For this study, I had access to a novel conditional aggrecan knockout mouse, allowing aggrecan to be knocked out selectively in local areas in the central nervous system, using the Cre-lox system. This allowed me to do a functional study on plasticity in the visual cortex of aggrecan knockout mice, the first of its kind. Ocular dominance (OD) plasticity is a classic manipulation for studies of activity-dependent plasticity where one eye is closed for several days (monocular deprivation). To assess the effect on OD plasticity I decided to use optical imaging of intrinsic signals, which provides a measure of neuronal activity in a whole brain area based on the hemodynamic response. The first part of my study consisted of setting up this method. Then, I proceeded to knock out aggrecan in the primary visual cortex (V1) of adult mice. The knockout was done by injecting Cre expressing adeno-associated virus in V1, which stopped the expression of aggrecan in this area. Following the injection, a monocular deprivation protocol was employed to assess the level of plasticity.

Histology was used to confirm viral transduction, and it revealed a strong reduction of PNN expression in V1. The plasticity assessments point towards an increased level of OD plasticity in the adult aggrecan knockouts, to a level that is similar to the high levels seen in juvenile animals. These results strengthen the hypothesis that aggrecan is essential for the PNNs in regulating the level of neuronal plasticity, at least in primary visual cortex.

Acknowledgments

I would like to give a big thanks to my supervisors, associate professor Dr. Marianne Fyhn and Dr. Torkel Hafting, as well as Dr. Gunnar Dick, for all their help and support throughout my work with this thesis.

A special thanks to Kristian Lensjø, who has contributed to several parts of this study, and who has always been willing to help. I would also like to thank the other members of the Hafting-Fyhn lab for always being available to answer questions and lend a helping hand, as well as Koen Vervaeke for the interesting and useful technical discussions.

Oslo, September 2015

Rune Alexander Lanton

Table of contents

1 Introduction

The nervous systems' ability to adapt and modify its function in response to changes in the surroundings is termed neuroplasticity. Neuroplasticity is essential to processes, such as development, learning and memory, and is crucial in recovering after damage to the nervous system.

Neuroplasticity occurs at many levels from changes in neurotransmission at the level of the synapse to the anatomical reorganization of neural networks. It can involve changes at the level of single synapses (Bliss and Lømo, 1973; Hughes, 1958), as the synapse itself is dynamic with the ability to be strengthened, weakened or even disappearing completely. This synaptic plasticity depend on the nature of the activity impinging on the neuron and the synapse. Plasticity changes can also take the form of large scale rewiring of cortical areas such as the restructuring demonstrated in the somatosensory cortex after digits amputation. Loss of input allows the cortical areas dedicated to the intact digits to take over the area previously assigned to the amputated digits (Merzenich et al., 1984). Furthermore, complete rewiring of large cortical areas has been demonstrated in e.g. blind people in which visual cortex is activated by the somatosensory input from reading braille (Sadato et al., 1996) and visual cortex has even been implicated in processing of auditory input (Thaler et al., 2011).

There is a striking difference in the level of neural plasticity between the juvenile and adult brain. In the juvenile brain, periods of heightened plasticity, critical periods, complete rewiring of connections after adequate sensory inputs are essential for the refinement of neural circuits into functional units. Plasticity is very much reduced in the adult brain and while the ability to change is vital, there is a need for stability in order to support long-term storage of information. Some brain areas retain their high level of plasticity throughout the life of the animal, while other areas become much less plastic. This variation points to mechanisms regulating the degree of plasticity in different areas of the nervous system.

One suggested regulatory mechanism controlling neuroplasticity may be specialized extracellular matrix molecules (ECM) called perineuronal nets (PNNs).

1.1 Perineuronal nets

The PNNs are ECM structures that wrap around certain neurons in several parts of the central nervous system (CNS). They were initially described by Camilo Golgi in 1893, but have until recently received limited attention. During the last couple of years, an increasing body of evidence has indicated that the PNNs are critical in regulation of neuronal plasticity (Carulli et al., 2010; Frischknecht et al., 2009; Pizzorusso et al., 2006, 2002; Wang and Fawcett, 2012).

Central components of the PNNs (figure 1.1) are hyaluronan, chondroitin sulphate proteoglycans (CSPGs), tenascin-R and link proteins (Carulli et al., 2006; Deepa et al., 2006). An important feature of the structure is the crosslinking of the components where the link proteins play an important role, binding hyaluronan and CSPGs of the nets together (Rauch et al., 2004). In fact, the link protein Crtl1 has been shown to be critical in the formation of PNNs. Transgenic knock-out mice, lacking Crtl1 in their PNNs, display attenuated PNNs in the cortex and retain juvenile levels of plasticity in the visual cortex (Carulli et al., 2010).

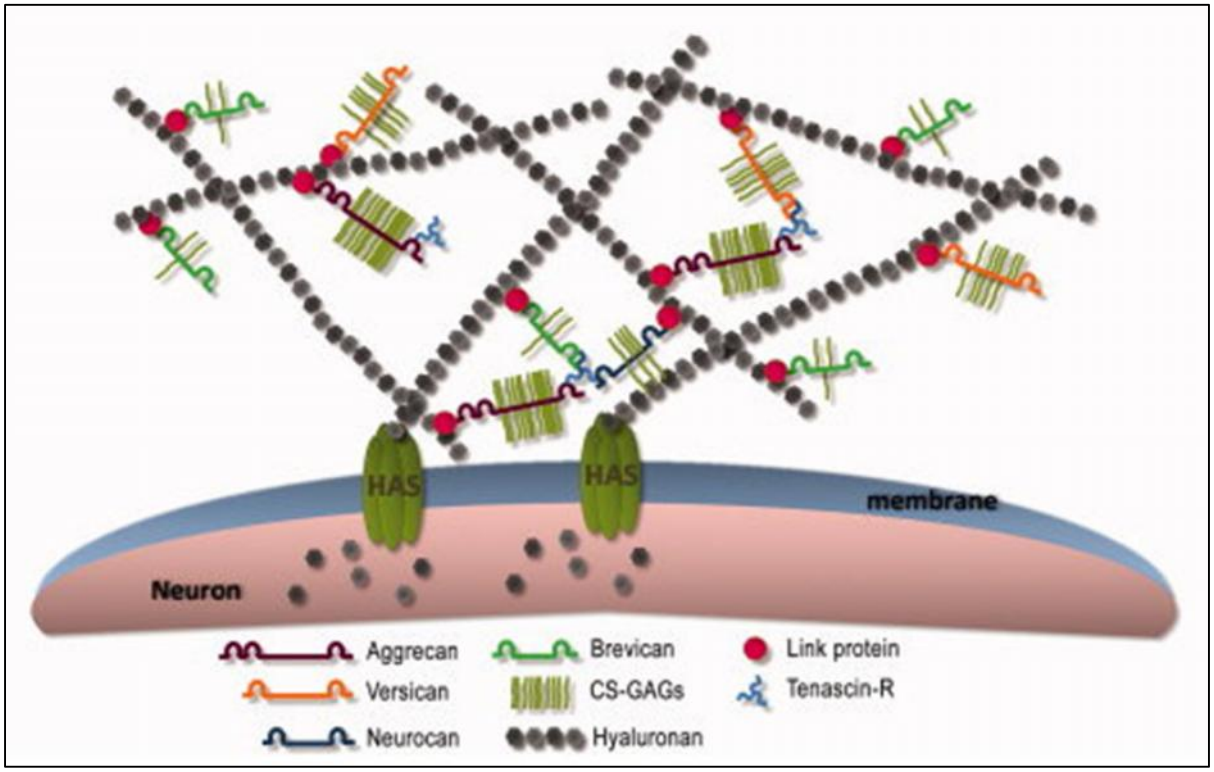

Figure 1.1 Showing the cross-linked structure as well as the individual components of the perineuronal nets. Adapted from Kwok et al. (2011)

Several different CSPGs, such as aggrecan, brevican and neurocan, may be present in the PNNs. The CSPGs consist of a core protein heavily saturated with glycosaminoglycan (GAG)

chains of chondroitin sulphate (CS). In principal, both the protein core and the glycan part of the CSPGs could contribute to plasticity regulation. The original finding that removal of CS GAG chains in the visual cortex of adult animals lead to regained plasticity (Pizzorusso et al., 2002), implicates the glycan moiety. Taken together, both the crosslinking of components and intact CS GAGs are essential for the functional PNN structure.

Due to the large CS content, the PNNs can be degraded by chondroitinase ABC (chABC), a bacterial enzyme that cleaves CS-GAGs of the CSPGs. Injection of chABC into the adult brain of rodents increases plasticity to a level similar to critical period levels of neuronal plasticity (Pizzorusso et al., 2002). However, the activity of chABC is not specific to PNNs, as CSPGs are abundant in the ECM in general. Thus, injection of chABC likely causes changes to the extracellular space and environment, not related to PNNs. Therefore, additional and more specific manipulations are needed to understand if, and how, the PNNs itself affect plasticity.

Several studies have shown that aggrecan is pivotal in the formation and function of the PNNs (Giamanco et al., 2010; Matthews et al., 2002; McRae et al., 2007). Aggrecan has therefore been suggested as a key player in regulating neural plasticity but this remains to be investigated in the intact brain.

1.2 Aggrecan

Aggrecan is a part of the lectican family of proteoglycans. It is a major constituent of cartilage throughout the entire body, but is also considered a key component of the PNNs. It is a large CSPG, with a mass of about 3MDa, consisting of a protein core that is decorated with about 100 negatively charged CS chains, in addition to several other oligosaccharides. Aggrecan interacts with hyaluronan and tenascin-R, effectively binding the PNN to the surface of the neuron (Morawski et al., 2012).

The existence of several different glycoforms of aggrecan in the brain (Matthews et al., 2002), could imply that different variants of aggrecan have distinct roles in plasticity regulation.

Aggrecan is the product of the *ACAN* gene, a gene essential for the organism due to the central role that aggrecan plays in cartilage. Mice lacking the functional *ACAN* gene, the *cmd* mice, will die at birth (Rittenhouse et al., 1978). Consequently, studies of brain plasticity in

global aggrecan knockout mice have been impossible. Previously, studies manipulating aggrecan in the PNNs were confined to *in-vitro* experiments (Giamanco et al., 2010). Aggrecan seem to be produced by the neurons themselves and not glial cells as many of the other components of the nets (Giamanco and Matthews, 2012). In the current project, I have had access to a novel conditional aggrecan knockout mouse, developed in the research group of Professor J. Fawcett (University of Cambridge, UK), enabling Cre-lox targeting of aggrecan limited to the CNS, thereby allowing investigation of brain plasticity in adult animals.

Descriptive *in-vivo* studies in mice have found that expression of aggrecan is activity dependent, with altered neuronal activity patterns leading to altered aggrecan expression (McRae et al., 2007). To test the role of aggrecan in neuroplasticity in the intact brain I chose to use a standard assay for activity-dependent plasticity: ocular dominance plasticity.

1.3 Ocular dominance plasticity

Normally, the binocular part, receiving information from both eyes, of primary visual cortex is more strongly activated by input through the contralateral eye as opposed to the ipsilateral eye. Such ocular dominance (OD) is a general phenomenon of mammals.

Seminal work by D. Hubel and T. Wiesel showed how altering the input to visual cortex by suturing the eyelids of kittens, resulted in changes to the OD distribution, termed OD plasticity (Wiesel and Hubel, 1965, 1963). They found that this monocular deprivation (MD) effect was especially strong in young animals, much more so than older animals (Hubel and Wiesel, 1970). This period of heightened sensitivity to such alterations were later termed the ‘critical period’. In mice, the critical period for visual cortex has been shown to center around 28 days after birth (postnatal day 28, P28), ending around P32 (Gordon and Stryker, 1996). In contrast, adult animals will not show such a shift unless they are exposed to a prolonged period of MD, typical more than six days (Sato and Stryker, 2008; Sternberg and Hamilton, 1981).

The OD plasticity has been the canonical system for investigations of cortical plasticity. The standard protocol involves measuring the pre-MD response of the contralateral and ipsilateral eye, then one or both eyelids are closed for a period, reopened and the responses measured

again. Based on the response strength of the two eyes an ocular dominance index (ODI) can be calculated.

Before optical imaging of intrinsic signals (OIIS) became available, the ocular response was measured using electrophysiological methods. However, due to its efficiency and non-invasive identity, the OIIS has more or less replaced other methods for routine OD characterization (Cang et al., 2005).

1.4 Optical imaging of intrinsic signals

OIIS is a method to infer neural activity. The method works by detecting changes in blood oxygenation and flow following neural activity, also known as the hemodynamic response, and was first described by Grinvald and co-workers (Grinvald et al., 1986). This signal, the blood-oxygenation-level dependent (BOLD) signal, is also the same signal that forms the basis for functional magnetic resonance imaging (fMRI).

The hemodynamic response is not fully understood, but what is known, is that increased neuronal activity in an area requires increased supply of oxygen and energy, resulting in an increased flow of oxygenated blood to activated neural tissue. The hemodynamic response has a rather slow time course, with even short periods of stimuli (< 2s) resulting in changes that last for >10s (Grinvald et al., 1986). The rise-time of the response is also quite slow, introducing a significant delay between stimulus onset and the measured response. This delay is called the hemodynamic delay.

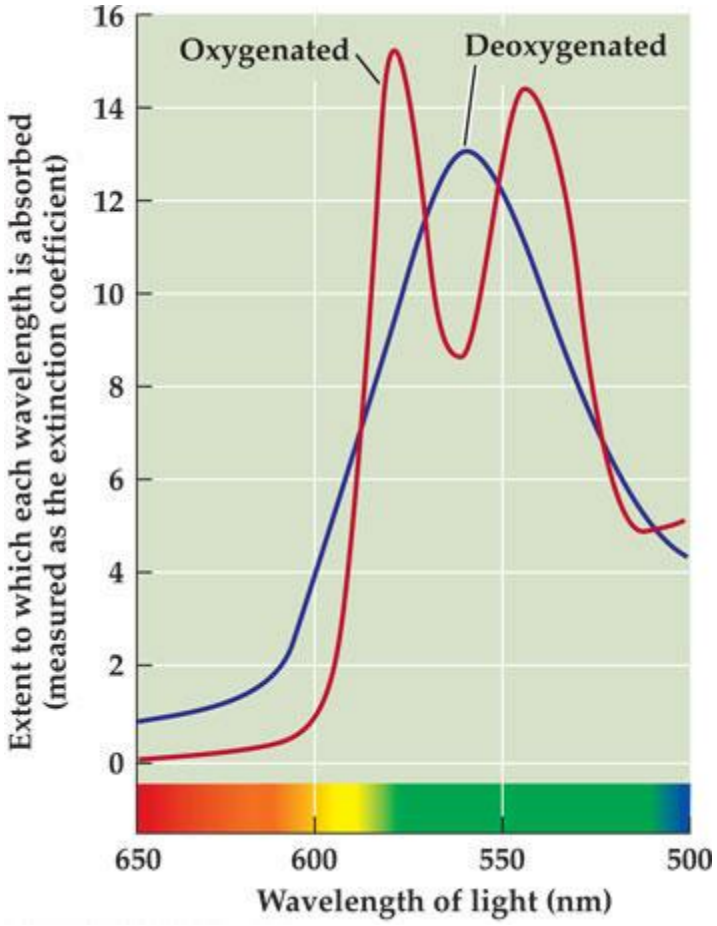

Figure 1.2 Absorption spectra of oxygenated and deoxygenated hemoglobin. From http://sites.sinauer.com/animalphys3e/boxex24.01.html.

By shining light on to the cortex and subsequently recording the reflected light using a camera, it is possible to determine the changes in blood flow and oxygenation level. These changes reflect changes in neural activity. As can be seen in figure 1.2, by choosing different wavelengths one can look at different aspects of the hemodynamic response. In some points, for example at approximately 590nm, or 550nm, the absorption is about the same. Conducting imaging at these wavelengths will provide information on blood volume, with little information on the oxygenation state of the blood. At other wavelengths, for example 600nm, or 560nm, the absorption is different between the deoxy- and oxyhemoglobin, resulting in changes to the level of oxygenation being detectable. Thus, imaging at these wavelengths will include an oxygenation level dependent component, in addition to the volume dependent component.

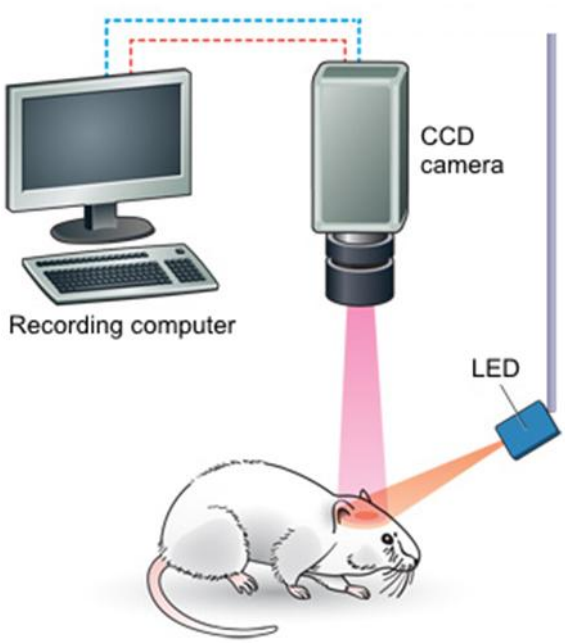

Figure 1.3 Setup for Optical Imaging of Intrinsic Signals. Activity in the tissue are recorded by shining light of specific wavelengths on to the exposed cortex and recording reflected light through a lens attached to a CCD camera connected to an acquisition system. See text for details. Adapted from http://www.bioopticsworld.com/articles/print/volume-5/issue-05/features/doubling-up-for-brain-imaging.html.

The complete setup is illustrated in figure 1.3. A camera, usually of the charge coupled device (CCD) type, is positioned above the head of the animal. Attached to the camera is a lens of some sort, usually a macroscope consisting of two regular lenses mounted face to face. This configuration gives an extremely narrow depth of field as well as a relatively long working distance and good brightness (Ratzlaff and Grinvald, 1991). The narrow depth of field helps to focus below the blood vessels at the surface of the brain, bringing them out of focus, reducing their impact on the recordings. In addition, a light source with the appropriate wavelength must be aimed at the cortical area. The most popular choice today is LEDs, which are cheap and can be found in many different wavelengths.

One challenge with OIIS is separating the stimuli induced response from biological background activity. The background hemodynamic activity changes constantly and it is influenced by factors such as respiration, heart rate, general state of the animal etc. Figure 1.4 shows the activity of a single pixel from a stimulus responsive region of visual cortex, notice the combination of lower frequency background activity and higher frequency stimulus induced activity.

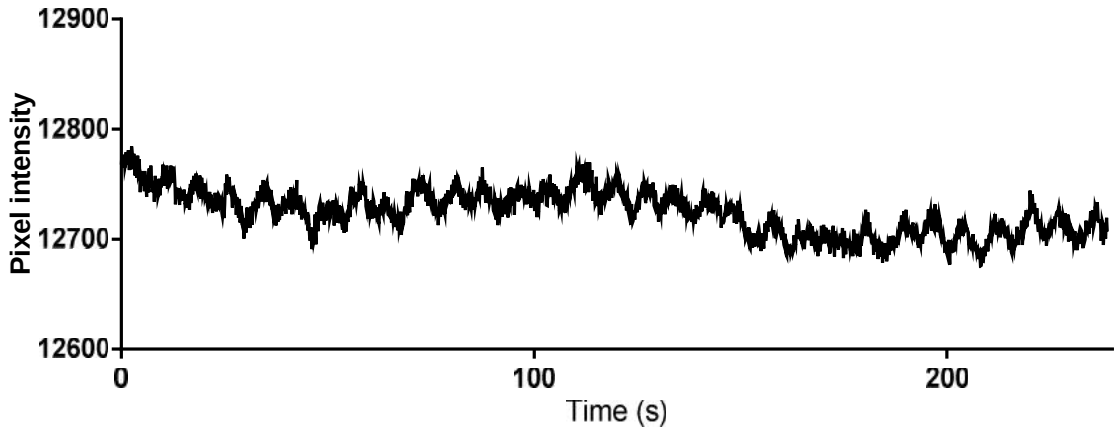

Figure 1.4 Pixel response during OIIS recording from a stimulus responsive region of visual cortex during visual stimulation (8s stimulation period).

Traditionally this problem has been addressed by presenting the chosen stimulus many times, doing a separate recording each time. The recording usually begins a few seconds before stimulus onset and continue for a few seconds after it has ended. All the recordings are then averaged together, the idea being that much of the background activity is more or less random and will cancel out, while the stimulus-induced response is not, and this will in turn give an improved signal-to-noise ratio. One can also generate pre-stimulus images that represent the background activity by averaging the frames taken before stimulus onset, and then subtracting these from the frames acquired during and after stimulus.

A different approach to counteract this problem was described by Kalatsky and Stryker (2002), where, instead of using episodically presented stimulus, they proposed to use a continuously running periodic stimulus. One would do one long, continuous recording while presenting a periodically repeating stimulus. To extract the response to the stimulus one would then employ the Fourier transform to generate a power spectrum (see figure 1.5), and by only considering the component at the frequency of the periodic stimulus one effectively filters out most of the background noise. In addition to the amplitude, the Fourier component also gives information about the phase of the signal. This phase information can in turn be used to determine the temporal aspect of the activity across the cortical area being imaged.

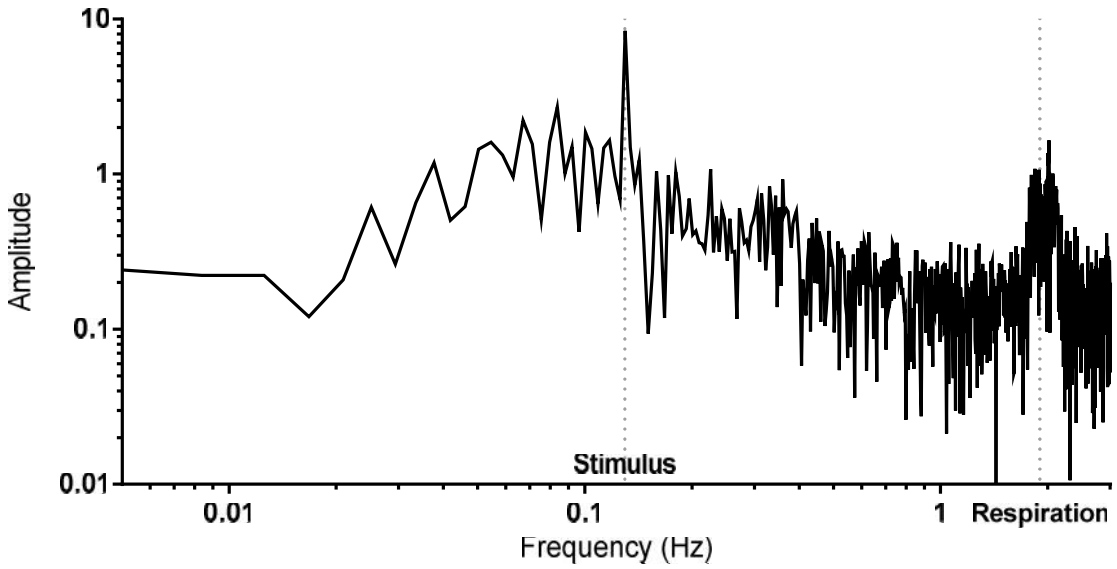

Figure 1.5 Typical FFT amplitude spectrum from stimulus responsive cortical area.

This approach has several advantages compared to the traditional method employing episodic stimuli. With this method, it is possible to generate detailed cortical maps of visual areas in as little as 2 to 4 minutes, a 100-fold reduction compared to electrophysiological or episodic methods (Kalatsky and Stryker, 2002). Replicating the high-resolution retinotopic maps using electrophysiological methods would also be extremely time consuming, if not impossible, to do. OIIS also allows the activity of large cortical areas to be measured with relatively little work.

The spatial, and especially temporal, resolution is quite low compared to other methods like electrophysiology, calcium imaging or voltage sensitive dyes. No data on the firing patterns or electrical potential of individual neurons are obtained, as the method is limited by the spatial and temporal properties of the hemodynamic response. The spatial resolution has been determined to be in the order of 250µm (Kalatsky and Stryker, 2002), and the temporal resolution is limited by the long duration, > 10s, of the hemodynamic response. Higher frequency signals will be present, but their amplitude will be greatly attenuated. However, OIIS is an ideal tool for investigations of cortical activation, such as in the case of OD and the effect of MD on visual cortical circuits.

1.5 Cre-lox recombination

The Cre-lox system was discovered in the P1 bacteriophage, where it plays an important part of the viruses' normal life cycle, being involved in circularizing the genome of the phage (Sternberg and Hamilton, 1981). Consisting of a recombinase called Cre, that catalyzes a recombination event between two loxP sites, and the loxP site, a specific 34-base pair genetic sequence, the system is not very complex. Introducing these two components into mammalian cells have been shown to allow controlled recombination events to take place (Sauer and Henderson, 1988) .

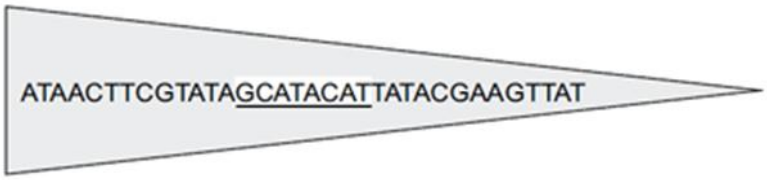

Figure 1.6 LoxP sequence, with an eight base-pair (bp) core sequence and two 13bp flanking inverted repeats. Figure from http://cre.jax.org/introduction.html.

The loxP sequence is shown in figure 1.6, and introducing a pair of these into a genome is all that is needed for the Cre-recombinase to affect a controlled recombination event. Depending on how the two loxP sites are placed and oriented different results can be obtained, this is illustrated in figure 1.7. The possible results are inversion of the sequence flanked by the two sites, the sequence can be deleted or the result may be a chromosomal translocation.

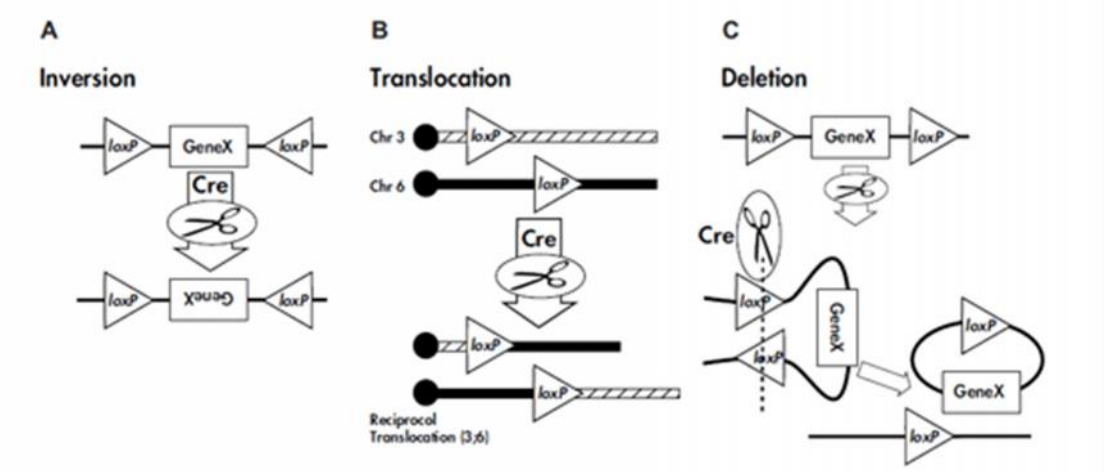

Figure 1.7 The orientation and location of the loxP sites determine the outcome of the recombination event. (A) Inverted loxP sites will result in the flanked sequence being inverted. (B) loxP sites on two different chromosomes will result in chromosomal translocation. (C) Two loxP sites oriented the same way will result in a deletion of the flanked region. Figure from http://cre.jax.org/introduction.html.

The most popular configuration is deletion, allowing one or more genes to be knocked out by introducing Cre into the cell. This is a very powerful technique for investigating the role of a gene or a gene-product.

Cre can be introduced into the cell in several different ways. One way is with the help of a mouse strain where a promotor sequence is used to express Cre in a certain cell type, or in a certain tissue. By crossing such a Cre strain with a strain containing a floxed gene, one will have recombination events restricted to the Cre expressing cells. It is also possible to engineer mouse strains with inducible Cre expression, where a non-functional form of Cre is produced until some inducing agent is administered (Garcia and Mills, 2002). Another approach involves introducing Cre by the way of local injections of a virus, allowing the researcher to introduce Cre in a local area under study. Several different families of viruses can be used, such as retroviruses, lentiviruses, adenoviruses and adeno-associated viruses (AAV). The most widely used virus for investigations of neuron circuits is probably the AAV serotypes. They cause very low immune responses and they are not known to cause disease in humans, making them less risky to work with compared to the other viral vectors, while still being highly effective for gene transfer (Kaspar et al., 2002).

Depending on what kind of promotor sequence is used in the viral vector it is also possible to narrow down the kind of cells that will express Cre, further increasing the usefulness of this method.

The combination of the Cre-lox system with viral vectors has increased the degree of control regarding where, and when, genes are knocked out, opened an avenue of novel opportunities for targeted genetic perturbations of neural function. It also solved several problems encountered in constitutive knockouts, such as non-viable offspring and compensatory mechanisms during development. Since the constitutive aggrecan knockout was lethal and previous investigations suggest that neurons are the source of PNN associated aggrecan, in the current study I used a conditional CNS specific knockout of aggrecan where exon four of the *ACAN* gene is flanked by loxP sites enabling Cre-dependent knockout of aggrecan. In order to restrict the knockdown effects I used local injections of AAV virus expressing Cre into visual cortex of adult mice to investigate the effect on plasticity.

1.6 Aim of study

The aim of my thesis was twofold.

1. Establish optical imaging of intrinsic signals as a method in the lab.

2. Use OIIS to examine whether knocking out the gene for aggrecan has an effect on ocular dominance plasticity.

2 Materials and methods

2.1 Animals

All laboratory work was done at the Department of Biosciences, Faculty of Mathematics and Natural Sciences, the University of Oslo. Before initiation, the experiments were approved by the Norwegian Animal Research Committee (FDU). The animal facility and the experiments with the animals are in accordance with the Norwegian Animal Welfare Act and the European Convention for the Protection of Vertebrate Animals used for Experimental and Other Scientific Purposes. All participants have completed a course in Experimental Animal Research (similar to a FELASA C course) and are approved by the FDU to conduct research experiments with animals.

The animals used for the study are transgenic C57BL/6 mice, developed in the laboratory of Professor James Fawcett (University of Cambridge, UK), by Dr. Gunnar Dick (Department of Biosciences). They have had loxP sites inserted into their genome, flanking exon 4 of the *ACAN* gene. This is the gene coding for aggrecan, allowing conditional knockout of aggrecan by the introduction of Cre recombinase. Two different strains, named G11 and F12, were obtained from Cambridge. Both strains have had the same genetic modification carried out, the only difference is that they originate from to different lines of stem cells, and both strains were used for this project.

Six female mice and two males were used. One of the females were heterozygous, all the others were homozygous. The animals were maintained on a 12/12h light/dark cycle (lights on at 20.00) and the temperature in the housing facilities were kept at approximately 21°C with humidity at 55 ± 10 %. The rooms have a ventilation rate of 5-20 times per hour. Mice were housed in groups of up to three, depending on sex, in polycarbonate cages (35x55x19 cm) with woodchip bedding (Scanbur, Karlslunde, Denmark). Food and water were available ad libitum throughout the period of experiments. Experiments were conducted during the light cycle.

2.2 Breeding and genotyping

The animals received from Cambridge were all heterozygous with regard to the genetic modification, necessitating the initiation of a breeding program to produce the homozygous animals needed for the study.

To determine the genotype of the animals, tail samples were analyzed using both PCR and genetic sequencing.

2.3 Virus injection

Anesthesia was first induced using a box containing a small amount of liquid isoflurane. After induction, the animal was placed in a stereotaxic frame and secured using ear bars. Gas anesthesia was maintained using a SomnoSuite (Kent Scientific, Connecticut, USA). The concentration of isoflurane was kept at approximately 2.6% and airflow at 100ml/min throughout the whole procedure. The animal was given subcutaneous injections (SC) of Atropine (0.03mg/kg) to prevent fluid buildup in the airways, and Rimadyl (carprofen 5mg/kg) as a general analgesic. Small drops of silicon oil was placed over the eyes to prevent desiccation. The animals' body temperature was monitored and maintained at 37ºC throughout the procedure using a MouseSTAT (Kent Scientific, Connecticut, USA).

The skin covering the skull was shaved, before the skin was cleaned using chlorhexidine. A longitudinal incision was made in the skin, allowing the skull to be exposed. A small craniotomy was made over the primary visual cortex (V1) using a dental drill. Coordinates used were 0.0mm anterioposterior relative to the lambdoidal skull suture and 3.0mm lateral to the midline suture.

Injections of viral vectors were carried out using a Nanoject II (Drummond Scientific Company, Pennsylvania, USA). The virus injected was AAV9.hSYN.HI.eGFP-Cre.WPRE.SV40 (Penn Vector Core, Univ. of Pennsylvania, USA). Cells transfected with this virus will express Cre recombinase and green fluorescent protein (GFP) as a reporter for transfection, under control of the synapsin promoter. This promoter leads to selective and strong expression in all neurons, but not glial cells, meaning that Cre and GFP will only be expressed in neurons. The concentration of the stock solution was $5.54 * 10^{13}$ GC/mL, this was diluted 1:10 before use. 500nL was injected in 10 injections, 50nL each, carried out over a total of 10 minutes. After the injections, the incision was sutured shut. The animal was allowed to wake up, and then put back in their cages.

The idea at the time of the injection was to proceed with experiments after approximately three weeks, but problems with getting the intrinsic imaging to work resulted in this period being extended to more than three months.

The procedure with injections was carried out in collaboration with Kristian Lensjø.

2.4 Head bar installation

In order to have the animals securely held in place during recordings, without causing any pain, a metal head plate was attached to the skull of each animal at the start of recordings.

The anesthesia and surgery procedures were the same as described above for viral injections.

The skin covering the skull was removed, and the bone surface cleaned off all organic residue. In order to protect the skull and keep it transparent for imaging a thin coat of liquid bandage (New-skin, USA) was applied to the bone covering the right hemisphere using a small brush. The rest of the exposed skull was covered in cyanoacrylate (superglue), allowing the dental cement to adhere more strongly.

A small amount of cyanoacrylate was applied to the head bar prior to installation, and the head bar was carefully placed in its correct position at the very anterior part of the exposed skull. Dental cement was used to fasten the head bar, all the time making sure the area of interest in the right hemisphere was kept clear.

Two different head bar designs were used for the experiments. For the first three animals, a head bar with a hole cut especially for imaging V1 was used. This was changed to a straight, more general-purpose design, for the last four animals. The reason for this change was that the straight bar placed anterior to the imaged area allowed a more uniform illumination of the area by blocking less light from the LEDs.

A small pencil mark was placed just posterior of the lambdoid suture at 3mm lateral of lambda, this mark was used during imaging as a reference point.

Animals were put back in their cages and allowed to recover for one day before pre-MD imaging and MD suture.

2.5 Monocular deprivation

At the day of monocular deprivation anesthesia was administered to reach a surgical level, approx. 2.5%. Then an injection of Rimadyl (carprofen 5mg/kg) was administered as a general analgesic and the contralateral eyelid was sutured shut. Three stiches was placed in the eyelid, one cross-stitch in the center in addition to two simple stitches, flanking the center stitch.

For the first three animals, an 8-0 suture (Ethicon) was used, but the animals seemed able to cut the thread using their claws. Because of this, the suture was changed to size 7-0 for the rest of the animals, a change that eliminated sutured eyelids opening prematurely.

The animals were then returned to the vivarium, where they were left to recover. The general state of the animals, in addition to the state of the sutures, where checked daily.

2.6 Visual stimulation

All visual stimuli were generated using a custom MatLab (MathWorks Inc., Massachusetts, USA) script. It was presented using PsychStimController, a MatLab based software package developed at the lab of Professor Michael P. Stryker (University of San Francisco, USA), built on top of the PsychoPhysics Toolbox (Brainard, 1997). The stimuli was presented on an 18” LCD monitor (Dell UltraSharp 1800FP) that was placed 25cm in front of the animal, as illustrated in figure 2.1.

Two different sets of drifting bars were used. Each set consist of a horizontal white bar, moving either upwards or downwards, on a black background. For one set, the bar was 10º high and drifted across the screen in 10 seconds. This set, the ‘slow bar’, was used for the first three animals. The second set, the ‘fast bar’, consist of a 5º high bar, drifting across the screen in 4.1 seconds, but having a period of 7.7 seconds. This means there was a period in which the screen was completely black. The rationale for this design was to have a fast moving bar, giving a strong response, but still being able to employ a period long enough that the hemodynamic response could keep up.

In order to measure ocular dominance the bar was only shown in the binocular visual field (20º of the visual field, and it was offset by 5º towards the contralateral eye (Cang et al., 2005)), this is shown in figure 2.1.

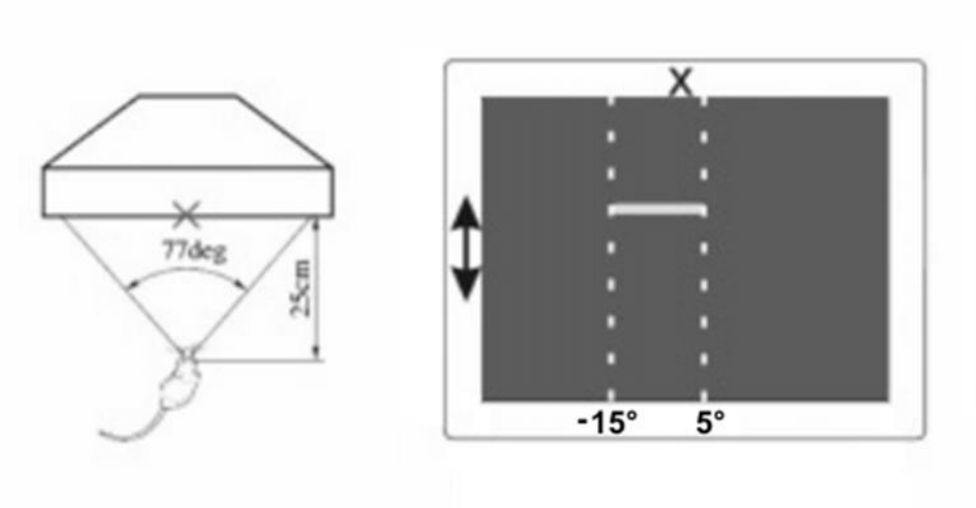

Figure 2.1 Setup for visual stimulation of anesthetized mice. Left; The animal was placed in front of the screen to secure a full field stimulation. Right; A white bar was moved up or down on a dark background in order to activate neurons in the visual cortex. In order to stimulate the binocular zone of the visual cortex, the white bar spanned 20º on the screen. Adapted from Cang et al., 2005.

The switch from the slow moving to the fast moving bar was made in an attempt to increase the strength of the stimuli induced response, thereby increasing the signal-to-noise ratio. The decision to change came from test recordings done on a separate animal. The faster rate of movement was intended to give a stronger response, and seemed to do so in the test animal. In addition, the change to a somewhat shorter period shifted the stimulus frequency to a slightly higher frequency, 0.13 Hz vs 0.1 Hz, moving the signal away from the low frequency biological activity.

2.7 Ocular dominance recordings

All recordings were done the through intact skull, the bone having been covered in a coat of liquid bandage after head bar installation (chapter 2.4).

Animals were anesthetized with isoflurane, 2.5% for induction and approximately 1.0% during recording. After induction, an intramuscular injection of Chlorprothixene (2 mg/kg) was administered, as well as a subcutaneous (SC) injection of Atropine (0.3 mg/kg). Chlorprothixene is a GABA agonist which has a sedative and anxiety reducing effect. The effect being that less isoflurane is needed during the experiment. Isoflurane has a strong depressive effect on neuron and glial activity (Hentschke et al., 2005).

The animal was secured in a custom-made frame via the attached head bar, and the whole setup was carefully positioned in center of the stimulus monitor. The distance between the eyes of the animal and the monitor was adjusted to 25cm (Figure 2.1).

The camera and lens was moved into position above the head of the animal, and by looking at the image coming from the camera, lowered into course focus. This was all done using the green LED in order to get a clear image of the blood vessels on the surface of the brain. Then the image was focused and panned into position using the fine adjustment micrometers of the setup. A short overview recording was made for later reference (1 second). The image was then cropped to the area of interest (AOI), with help of the reference mark made during head bar attachment, and a short surface recording (1 second) was made.

Then, a block, made of cardboard and fabric, was placed between the eyes of the animal and the exposed skull. This block served two purposes, it prevents light from the monitor hitting the skull and contaminating the recordings, and it prevents the animal from being blinded by the LEDs.

The illumination was switched from the green LEDs (525nm) to the red LEDs (615nm). The focus was moved approximately 650um below the cortical surface and a 180 seconds recording was carried out using visual stimulus spanning the full screen (71º). This first recording allowed the verification of the correct AOI.

The stimulus was changed so the bar only spanned 20º, the binocular area, and a couple of 180-second recordings were made, trying all the time to assess the stability of the animal. When subsequent recordings looked stable enough the OD recording routine was started.

A small plate of cardboard and tape was used to alternatingly block input to the ipsilateral and contralateral eye.

For the first three animals, the block was left in place for two consecutive recordings, one with the bar moving up and one with the bar moving down. This was done to minimize the number of times the block had to be moved, as each move involved a risk of disturbing the setup. Six recordings were made for each eye, resulting in 12 recordings total, each 4 minutes long.

For the last four animals, the block was moved between each recording, and the first six recordings were done with stimulus moving down, while the subsequent six recordings were made with stimulus moving up. The block was not moved when switching from downwards to upwards stimulus, allowing the series to start and end with the same eye. This was done to counteract any effect of response strength changing with time. Again, the total number of recordings for one session was 12 recordings of 4 minutes.

Recordings were carried out just prior to MD sutures (day 0) referred to as the pre-MD recording (Figure 2.2). Then another recording session was carried out immediately following removal of MD sutures, the post-MD recording. Extra attention was given to this recording, making sure the sutured eye stayed open during the entire recording session. Recording sessions were also carried out for most animals at 2 days, and some, 4 days, and 7 days after removal of the MD sutures. The timeline of the whole experiment is shown in figure 2.2.

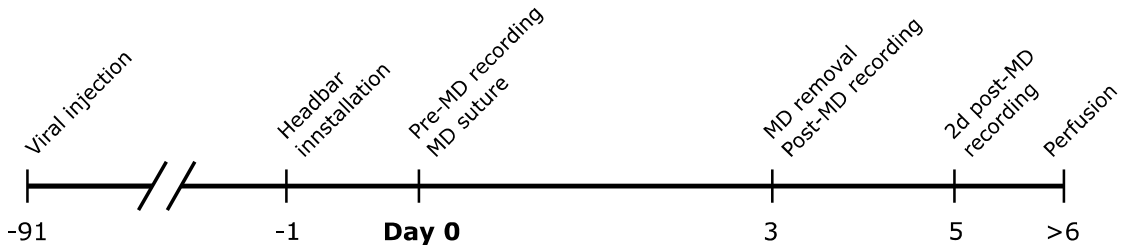

Figure 2.2 Experiment timeline.

To quantify the ocular dominance an OD index (ODI) was calculated:

ODI = (ResponseContra - ResponseIpsi) / (ResponseContra + ResponseIpsi).

ResponseIpsi and ResponseContra was found by first filtering the amplitude image for the given eye by a 5x5 filter, and the responsive area was defined as the area of the ipsilateral response image stronger than 60% of the max value. Then the strongest response of this area was used as the response for the eye. The ODI ranges from -1 to 1, where a value of 1 means complete contralateral dominance, while a value of -1 means complete ipsilateral dominance.

2.8 Histology

2.8.1 Perfusion

Animals were initially chamber-anesthetized using isoflurane, before being given an intraperitoneal injection of pentobarbital sodium (25 mg/kg). When no longer responding to a toe pinch, the animal was transcardially perfused with 0.9% NaCl in 1M phosphate-buffered saline (PBS) followed by 4% paraformaldehyde (PFA) in 1× PBS. The brain was then dissected out and post-fixed in 4% PFA. The tissue was transferred to a cryoprotective 30% sucrose solution in 1× PBS at 4°C for at least 24 hours in order to dehydrate the tissue before freezing. The tissue was flash-frozen and cut into coronal sections, 40µm thick, using a cryostat (Ortomedic, Lysaker, Norway).

2.8.2 Staining

Staining for PNNs was performed using *Wisteria floribunda* agglutinin (Sigma-Aldrich, Munich Germany) and an antibody against aggrecan (AB1031, Merck Milipore, Darmstadt, Germany). We additionally stained for GFP (anti-GFP, Abcam, Cambridge, United Kingdom) in order to visualize the area infected by the virus.

All sections were stained while free-floating in solution. The sections were collected from the cryostat and rinsed in 1× PBS. Sections were blocked in 1× PBS containing 1% bovine serum albumin and 0.03% Triton x-100 for one hour, and incubated with WFA in blocking solution overnight (1/200 dilution). On the following day, the sections were rinsed in 1× PBS, and incubated with the other primary antibody (anti-GFP or AB1031) in blocking solution overnight (1/1000 dilution). On the third day, sections were rinsed with 1× PBS and incubated with secondary antibodies in 1× PBS for two hours (1/2000 dilution), rinsed in 1× PBS and ddH20 and mounted on Superfrost Plus slides with FluorSave anti fading agent (Merck Milipore, Darmstadt, Germany).

2.9 Optical imaging of intrinsic signals

2.9.1 Hardware

I developed the OIIS setup based on the setup described in the paper by Kalatsky and Stryker (2002).

The workshop at the Department of Biosciences built a mechanically stable apparatus for mounting the camera and lenses according to my specifications. It consists of a vertical column, mounted to a foot, which can be magnetically attached to a work surface. On this column is a movable arm for mounting the camera as well as the lenses. The arm can be moved vertically along the column, allowing course focusing. At the end of the arm are three micromanipulators, allowing fine movement of the camera and lenses in all three directions. The workshop also built an adapter allowing two normal camera lenses to be mounted face-to-face, using the filter mounts on the lenses. The setup is shown in figure 2.6.

Two Nikon 50mm, 1.2 lenses were acquired, and mounted face-to-face, creating a macroscope with a 1:1 magnification.

The camera is a critical component of the setup, and the most important characteristics of the chosen camera is high well depth, at least 12-bit digitizer and decent resolution.

Using a camera with a high well depth is critical to overcome the shot noise. Shot noise is noise caused by the random nature of the arrival time of photons on the detector, and it is equal to the square root of the number of captured photons. Meanwhile the signal we are trying to capture is approximately 1/1000 of the total number of captured photons. Figure 2.3 shows how the signal-to-noise ratio (SNR) changes as a function of well depth.

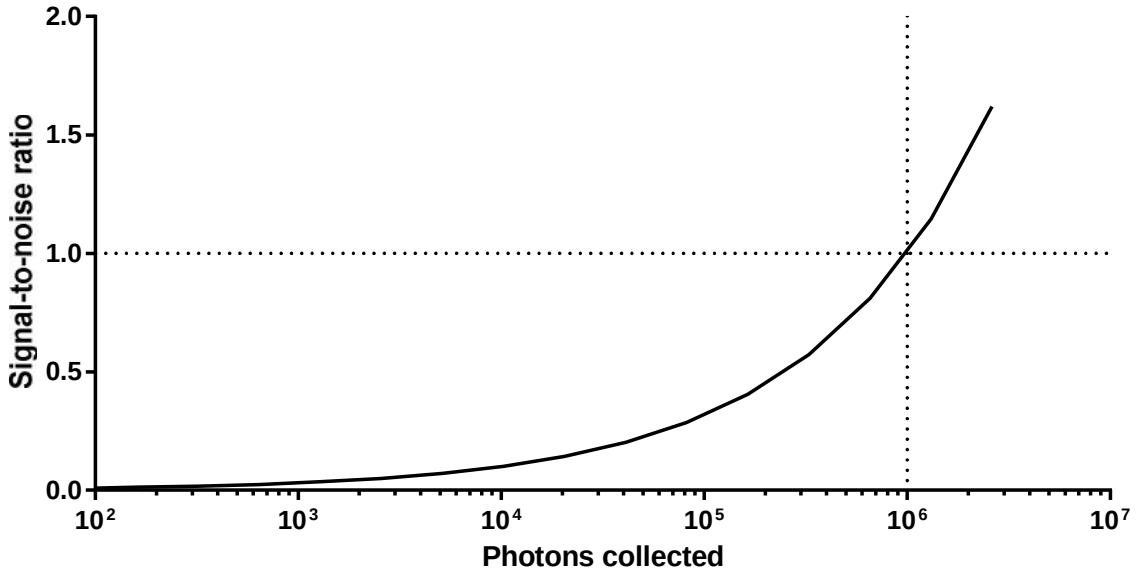

Figure 2.3 Shot noise and the effect of the cameras well depth on signal-to-noise ratio.

Many modern CCD cameras have well depths on the order of 20ke$^-$ or less, and it can be seen that quite a lot of frames would have to be collected to overcome the shot noise with such a small well depth. From figure 2.3, it is clear that >1000000 photons need to be collected to achieve a SNR of one, meaning 50 frames at 20ke$^-$ per frame. That is before we consider any other sources of noise affecting our SNR.

The 12-bit digitizer, allowing 4096 levels of intensity to be encoded, makes it possible to capture the tiny changes in light intensity on top of a large signal. Many cameras only use an 8-bit digitizer, allowing only 255 levels of intensity to be decoded. This can also be alleviated by averaging several frames, but this puts additional load on the recording system.

The quantum efficiency is of less importance since this method is not limited by the amount of available light. The same goes for other sources of noise, like thermal and electrical, that are critical in cameras used for light-starved applications.

The choice of camera fell on a used 1M30P (Teledyne Dalsa, Ontario, Canada). The camera, along with the power supply (DALSA-PV-UNI, Teledyne Dalsa, Ontario, Canada) were sourced from eBay. Both items, being second hand, had partly defective fans, making a lot of noise, so both fans were replaced. The camera is a black and white CCD camera, having a resolution of 1024x1024 pixels and employing 12-bit digitization. Maximum framerate is

129fps. The high well depth, 200000 electrons, in addition to the 12-bit digitizer, makes this camera well suited for the task.

The camera utilize a proprietary parallel low-voltage differential signaling (LVDS) based interface, so an image acquisition board (PCI-1422, National Instruments Corporation, Texas, USA) also had to be sourced from eBay. This board allowed the camera to be connected to the recording pc, but first a custom cable had to be constructed. The cable was built from a standard SCSI2 cable and the correct connectors, all acquired from DigiKey (Digi-Key Corporation, Minnesota, USA), and then soldered by hand according to a connection diagram sourced from National Instruments.

A stable light source is of course critical for this method. Since the whole concept relies on measuring changes in light intensity, any intensity fluctuations in the light source will directly affect the recorded signal. Especially critical is fluctuations at or around the frequency of the stimulus.

For the light source two different LEDs from Thor Labs, one at 530nm (M530L2, Thor Labs Inc, New Jersey, USA) and one at 625nm (M625L2, Thor Labs Inc, New Jersey, USA), as well as a power supply, was tested. However, the large size of the LEDs, as well as the fact that we only had one of each wavelength, made it very difficult to achieve even illumination of the cortex.

I therefore decided to build a custom lighting system. Inspired by the ring-flashes used for macro photography, the system was built by cutting a piece of thin sheet metal into a ring formed shape, with 5 small ‘flaps’ for mounting LEDs, these flaps could then be bent inwards to get the correct angle for the LEDs. Then individual LEDs, and the necessary mounting plate (804090, Bergquist Company, Minnesota, USA), was acquired, the LEDs soldered to their plates, and then mounted to the sheet metal with thermal compound and screws. Three 615nm LEDs (XPEBRO-L1-R250-00B02, Cree Inc, North Carolina, USA) and two 525nm LEDs (XPCGRN-L1-R250-00703, Cree Inc, North Carolina, USA) were used, the 525nm LEDs being used for surface images, while the 615nm being used for doing intrinsic imaging. All the LEDs were wired up and then connected to a switch allowing the light to be switched between no light, 525nm or 615nm. The illuminator construction is shown in figure 2.4.

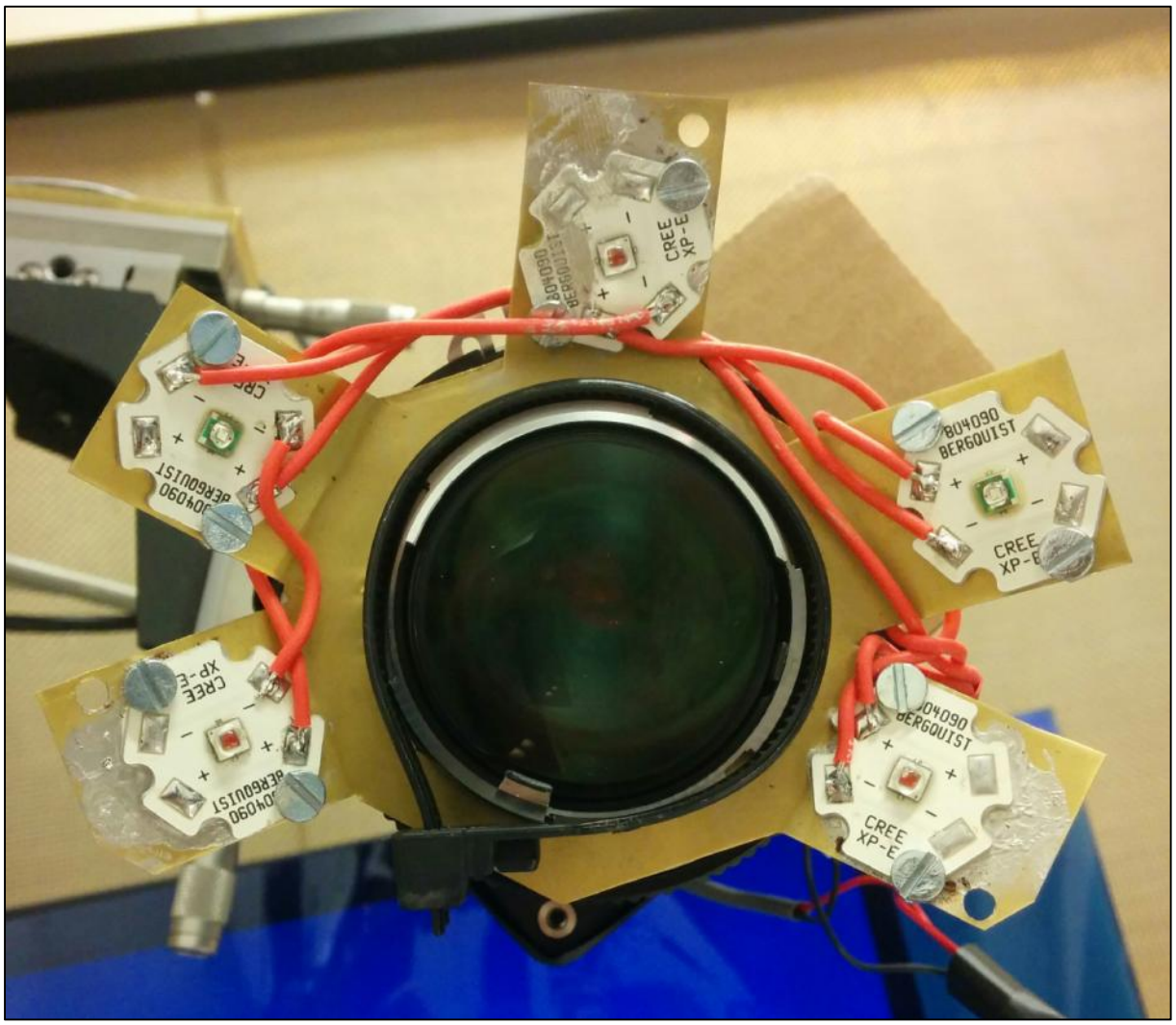

Figure 2.4 Custom built light source for illumination of the cortex during recording of cortical activity.

A custom, low noise constant current power supply for the LEDs was also constructed, being vital to get stable illumination. However, this turned out not to be enough, as LEDs change their light output with temperature. Some measures where tested to counteract this, but the only way to solve this is by employing some form of feedback, using for example a photodiode to regulate the power delivered to the LEDs. Nevertheless, tests also showed that the changes in illumination due to thermal effects were so slow that they did not interfere very much with the intrinsic signals. Therefore, no further measures were employed to address this.

One critical point when doing OIIS in combination with visual stimulus is blocking stray light from the stimulus monitor from being picked up by the camera. This light would show the same temporal characteristics as the stimulus induced response, and would therefore degrade the signal to noise ratio if allowed to reach the camera. To solve this a band pass interference filter, centered at 610nm, 10nm full width-half max was acquired from Edmund Optics

(43183, Edmund Optics, New Jersey, USA). The placement of the filter had to be carefully considered, since the angle of incidence alters the passband of an interference filter, so the optimum placement would be where rays of light were parallel. The only place in this setup where this is the case is between the two lenses. The necessary components for building a filter housing between the two lenses were acquired from Thor Labs. The filter also had to be removable, or else imaging using the 525nm LED would be impossible.

In addition to the interference filter, a cheaper colored plastic filter was placed in front of the stimulus monitor. This filter, functioning as a notch filter, blocks light around 600nm, while at the same time allowing shorter and longer wavelengths to pass. This filter was acquired from FotoVideo Norway AS (FotoVideo Norway AS, Oslo, Norway). Studies have shown that mice are not particularly sensitive to light above 600nm, so introducing such a filter should not affect what the mouse sees to any large extent (Jacobs et al., 2004).

In combination, these two filters blocks most of the stray light coming from the monitor, light that otherwise would reduce the signal-to-noise ratio of the recordings. One simple test, done by placing a piece of paper at a 45º angle to the monitor beneath the camera while presenting the drifting bar stimulus, showed that these two filters in combination block > 98% of all stray light coming from the screen, the measurements are shown in figure 2.5. The dotted line marks the approximate level of the stimulus-induced responses, > $1.0 * 10^{-4}$, indicating that both filters are needed to obtain a decent SNR at these levels.

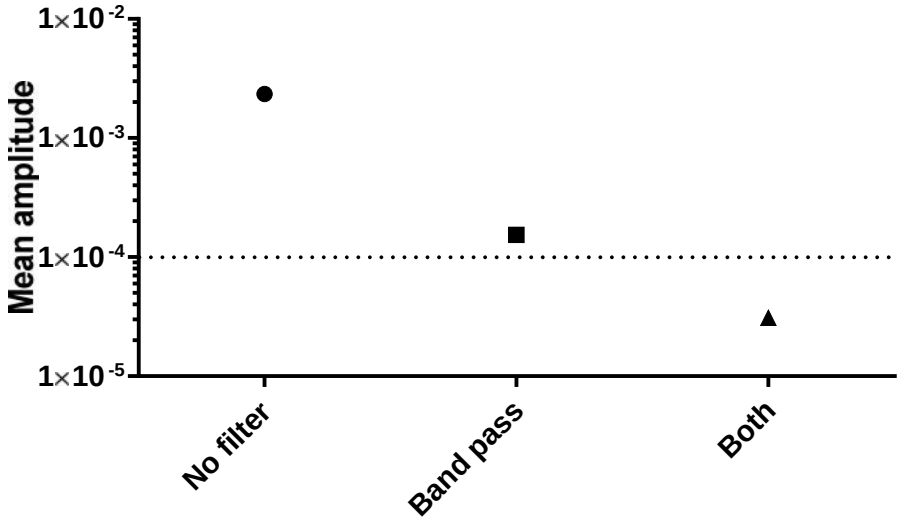

Figure 2.5 Effect of filters on stray light. The dotted line marks the magnitude of the stimulus-induced response. Notice the logarithmic y-axis.

The finished OIIS setup is shown in figure 2.6.

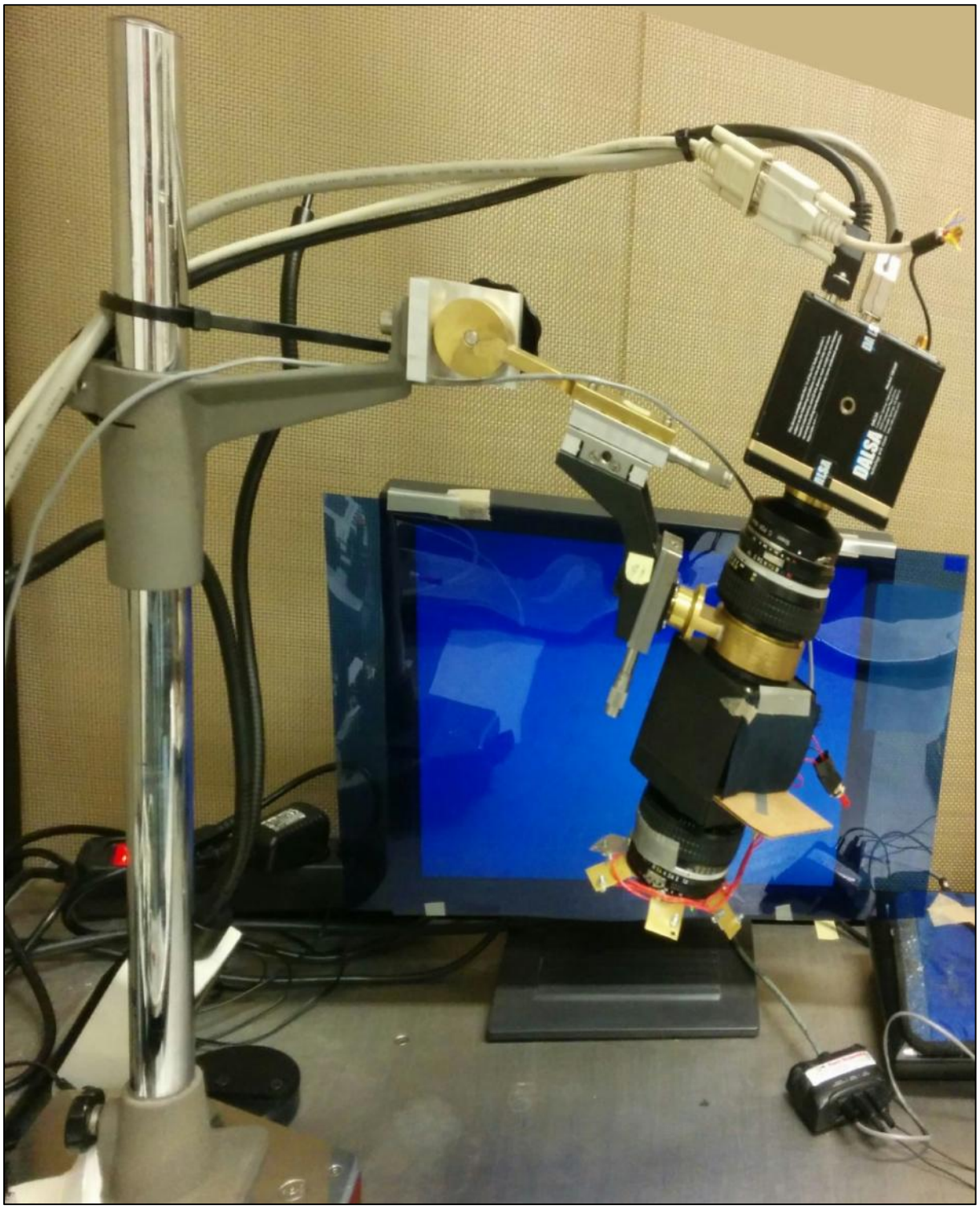

Figure 2.6 Complete OIIS setup, showing the stand with the magnetic base as well as the camera and the lenses. The switch for choosing the wavelength of the illumination is also visible.

2.9.2 Software

An image capture program was written in C++ using LabWindows, a part of the LabView package from National Instruments (Figure 2.7). This allowed the use of the IMAQ drivers from NI, greatly simplifying the whole process of capturing image data from the camera. The program only includes basic functionality, allowing framerate and shutter speed to be changed. It includes a preview function as well as a histogram view, helping to assess illumination quality. The program also includes the possibility of cropping the recorded video, allowing only the region of interest to be recorded, reducing the disk space taken up by the recordings. Pixel binning was also implemented in software, requiring the use of multiple threads to extract the necessary performance. The camera do support hardware binning, but the combination of hardware and National Instruments drivers made the use of this function very difficult. The software implementation, while being more resource heavy on the recording computer, should prove optimal in terms of signal quality given that hardware binning often is restricted in terms of total electron capacity of readout buffers in the CCD chip.

The image capture program creates a separate folder for each recording, and writes all frames to the disk as TGA files. Metadata about the recording is written to a separate text file that can be read in later by the analysis software, containing information on things like framerate, shutter time, time of first frame, time of last frame and number of captured frames.

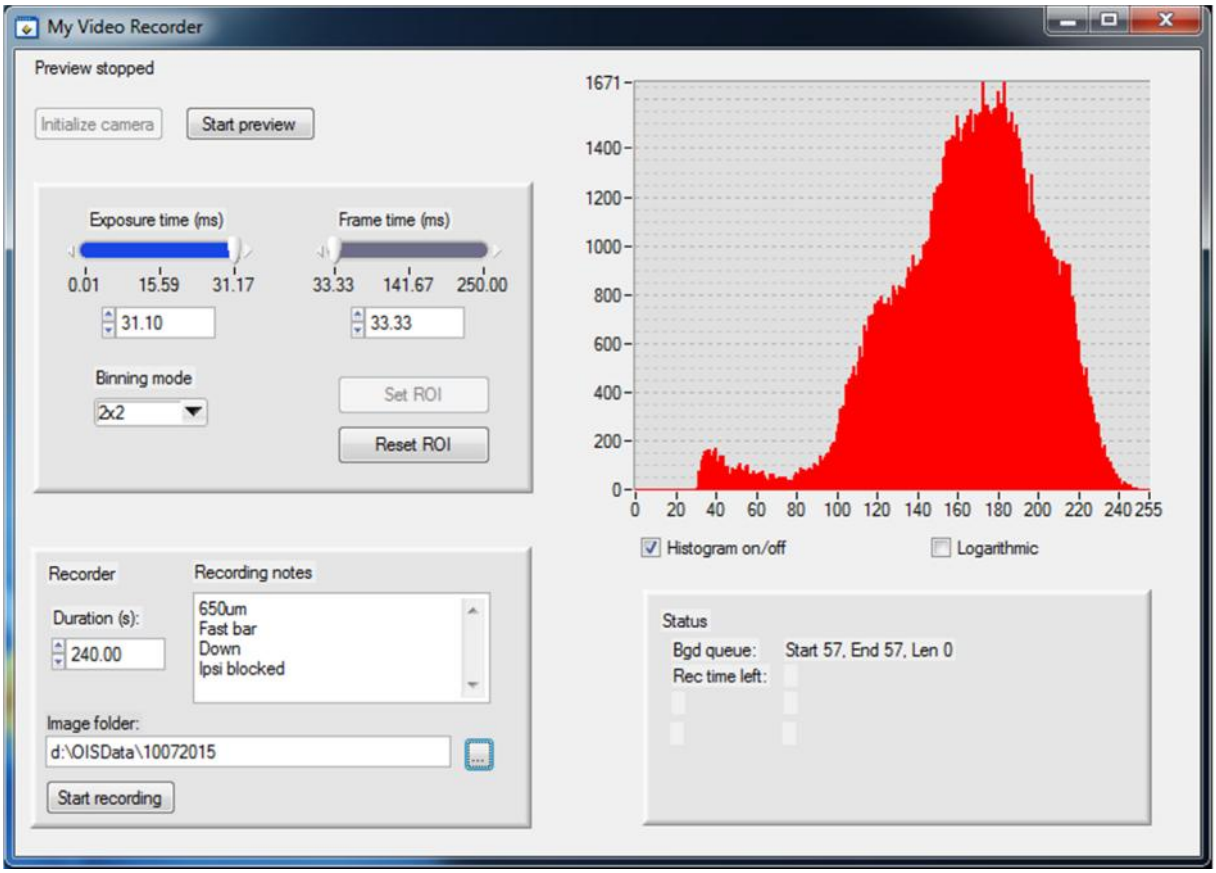

Figure 2.7 Image capture software.

Another small piece of software, a UDP server, was written in C# using Visual Studio from Microsoft. Its task is receiving synchronization data from PsychStimController. allowing images acquired to be synched with current state of stimulus presentation. This is necessary given that the software for presenting stimulus and the software for image acquisition is running on separate computers. The use of UDP packages sent over the local network through a single network switch allows the two events to be synched to within a couple of milliseconds, good enough for this task. The whole UDP server functionality should probably be moved into the image acquisition software, this would make the whole setup easier to use, with less chance of errors.

The third piece of software developed consist of a set of MatLab scripts along with a graphical user interface (GUI) (Figure 2.8). This is the scripts responsible for analyzing the data, reading in all required files, applying the FFT transform and extracting the response. The software generates images showing the absolute amplitude of the response, the relative change in light intensity as well as a phase map.

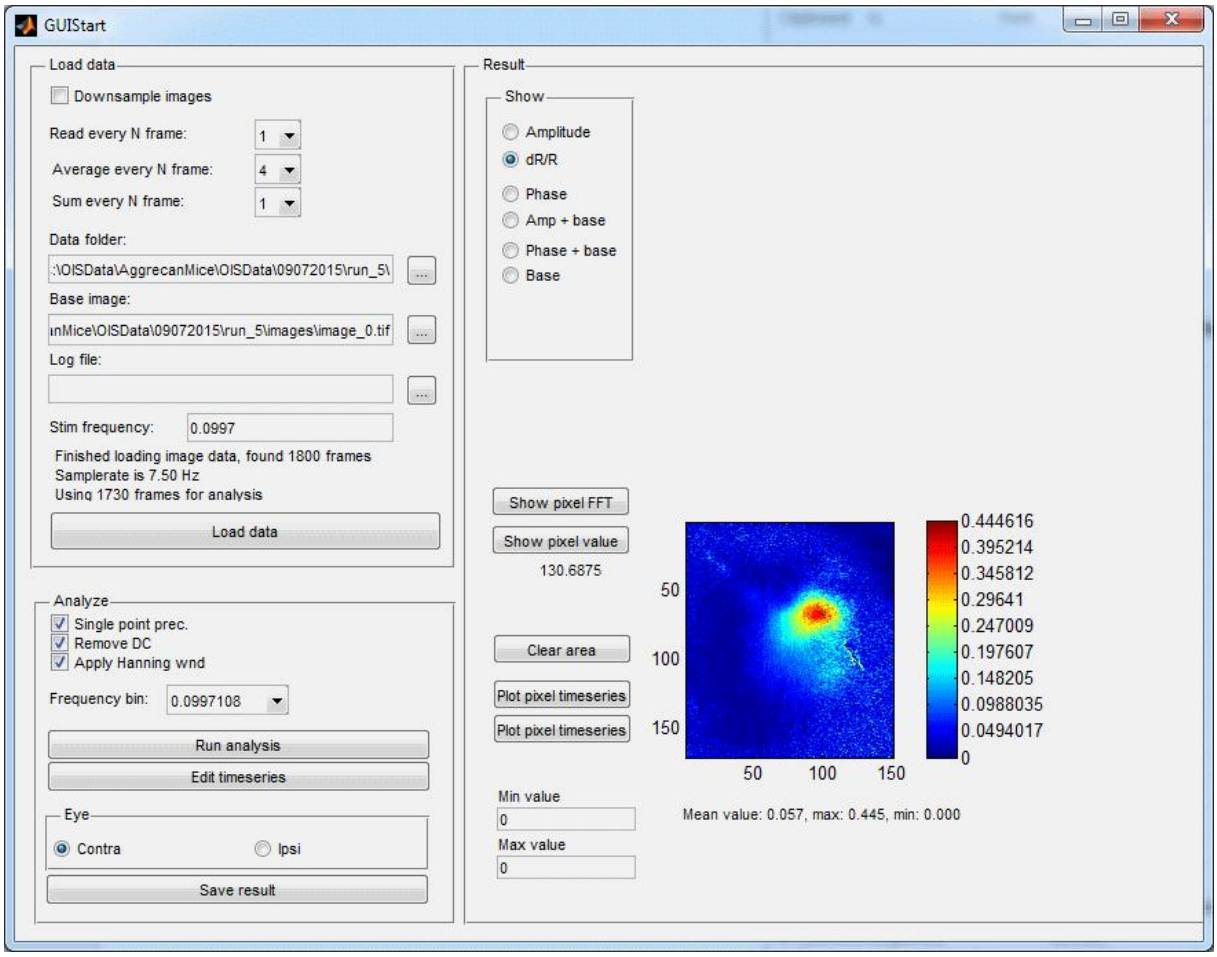

Figure 2.8 Analysis software.

This software allows data to be binned both temporally and spatially, again to improve the SNR. For all analysis done in this thesis, four frames were temporally binned, reducing effective sampling rate from 30Hz to 7.5Hz. Another important aspect of this software is that it adjusts the number of frames used for the analysis so that it is as close to a whole number of stimulus periods as possible. This is important for getting correct phase information. Before doing the FFT transform the software also removes slow changes in the recorded data by high pass filtering.

3 Results

3.1 Optical imaging

The first part of my thesis work consisted of setting up the method, and verifying that everything worked the way it should.

I chose to test the OIIS setup in a stepwise manner. This was done to make it easier to identify and fix any issues that would occur. After having the basic hardware, as well as functioning software up and running, a simple blinking LED was used for the first tests. The LED was covered by a neutral density filter (NE530B, Thor Labs Inc, New Jersey, USA) with an optical density of 3.0, meaning it has a transmission value of 0.1%. The use of such a filter allowed me to attenuate the signal to a realistic signal level. The intensity of the LED was modulated using a sine function at several different frequencies, in the range of 0.10Hz to 0.13Hz, approximating the changing signal I would later record in real subjects. This simple setup allowed me to test both the recording system, including hardware such as the camera and the lenses, as well as the software for acquiring and storing data. It also allowed me to test the function of the analysis software. This setup allowed me to verify that the setup was able to detect the weak signal from any background signals.

One challenge that I came across during this early testing was the stability of the LED light source. The intensity would drop of during a recording session, as shown in figure 3.1, and some time was spent trying to rectify this. However, this turned out to be less of a problem than I first feared since the changes were so slow that it did not affect the recordings. The intensity would also stabilize over time, with the LEDs reaching a thermal equilibrium with the surroundings. Nevertheless, some fluctuations remained.

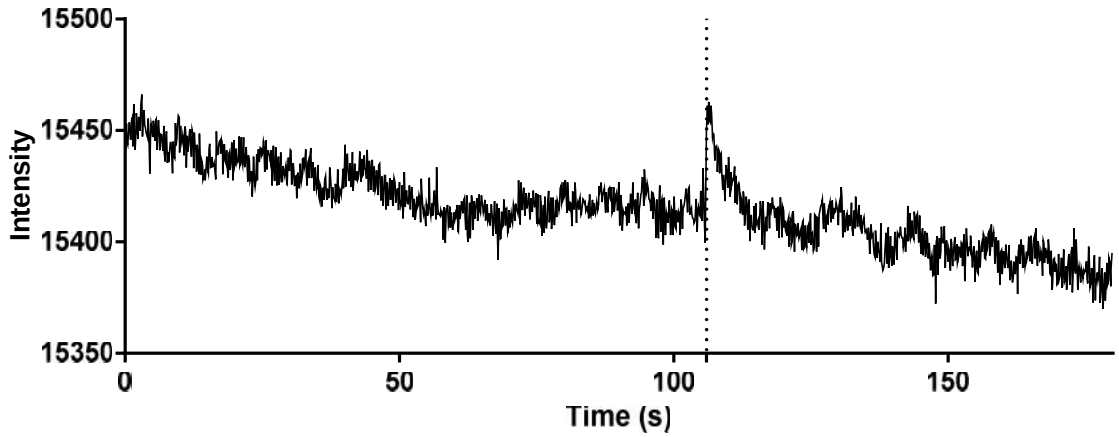

Figure 3.1 Light intensity of LEDs dropping over time. With a spiking event visible at about 106 seconds.

After testing and improving both software and hardware using the artificial signal source, I went on to test the setup on anesthetized mice. These tests uncovered several new challenges, the most severe being the problem of evenly illuminating the subject without creating any undue highlights. This lead to the design of the ring-light shown in figure 2.4. The ring-light did improve matters tremendously.

Figure 3.1 also illustrate another challenge I encountered with mice, sudden spikes in the intensity. A high percentage of all recordings would contain a relatively strong and fast rise in intensity, which would then drop back to baseline over the course of a few seconds. These spiking events do degrade the quality of the recording and quite a lot of time was spent trying to get rid of these. It turned out that by changing the posture of the animal, by lowering the body of the animal in relation to the head, the occurrence of such spiking event was almost eliminated. I also implemented a function in the analysis software that could be used to reduce the impact of such events.

Another challenge was stray light from the stimulus monitor being picked up by the camera, decreasing the SNR of the recordings. This was solved fully by the introduction of an interference filter in between the lenses and a band pass filter in front of the monitor, as described in chapter 2.9.1.

The recorded signal is contaminated with biological background activity in addition to the stimulus-induced signal, as shown in figure 3.2A. The background activity follows a 1/f distribution, meaning the power of the signal decrease with increasing frequency. To remove as much as possible of this low frequency background activity, as well as to remove most of the DC shift, the raw signal is high pass filtered by subtracting a low pass filtered version of

the raw signal from the raw signal. The result of this is shown in fig 3.2B, and it is clear that the low frequency content is more or less gone. The signal has also been shifted down to an average value of close to zero, removing most of the DC shift of the raw signal. Due to the way the Fourier transform works, any uncorrected DC bias will lead to both amplitude and phase information being incorrect.

To illustrate the point that the variations are of the same frequency as the presented stimuli, figure 3.2C shows a low pass filtered version of the time series, overlaid with a cosine of the same frequency as the stimulus, and after shifting the fit becomes obvious.

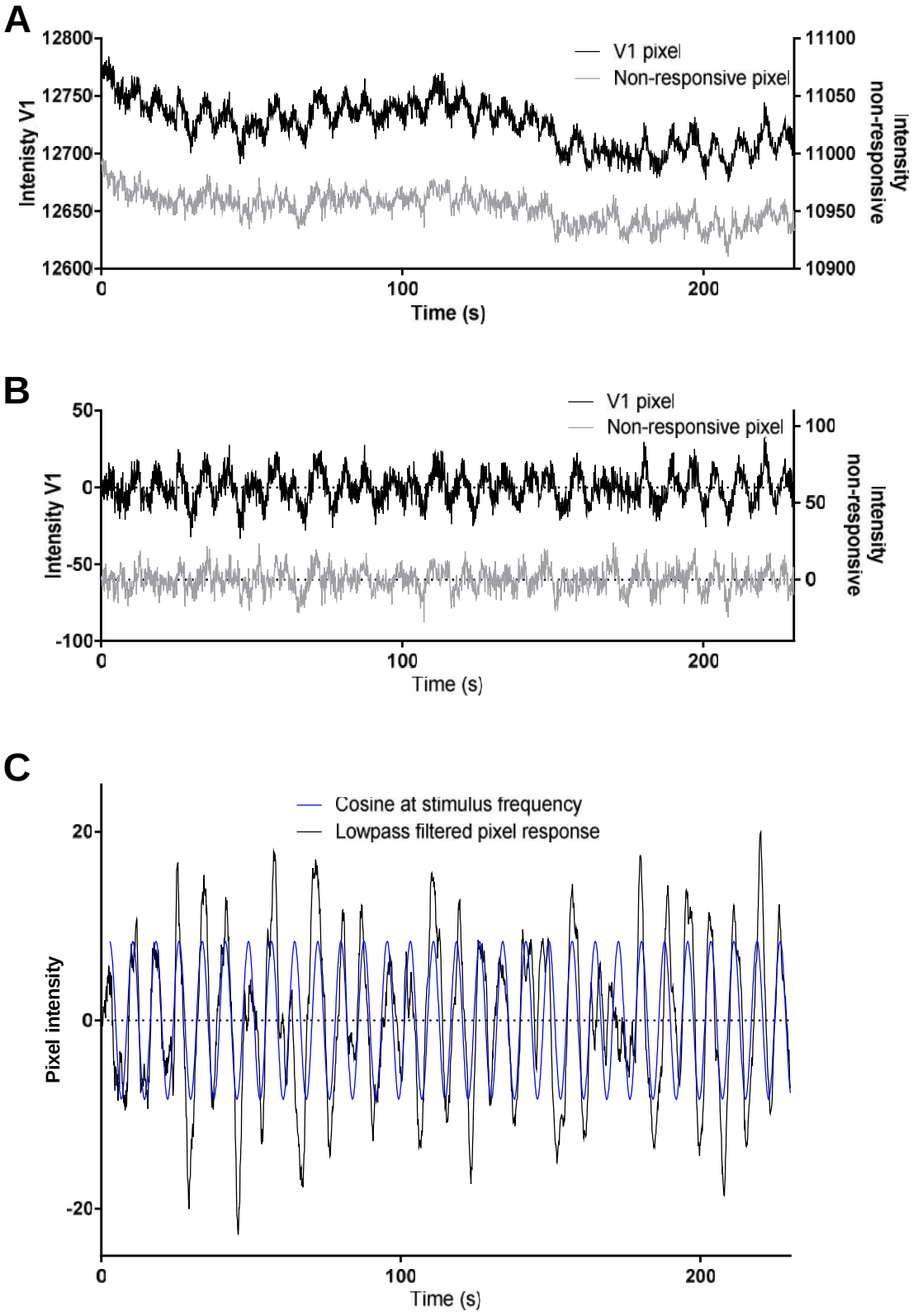

Figure 3.2 Example of a time series for a pixel located in V1 and one located in a non-responsive region. (A) Raw values of a selected pixel for a full 240 sec recording session. (B) Intensity values of (A) after high pass filtering to remove the slow variations of the signal. (C) Low pass filtered version of (B), with an overlaid cosine of the same frequency as the stimulus presented to the animal. Cosine has been phase shifted to match recorded signal.

An amplitude spectrum, calculated from the high pass filtered signal in fig 3.2B, is then created using a Fourier transform, as shown in figure 3.3.

The spectrum clearly shows the peak at the stimulus frequency of 0.1296Hz, with decent SNR. A smaller peak around 2Hz, caused by the respiratory activity of the animal, is also visible. The dip in the spectrum above 0.1Hz is caused by the earlier described high pass filter, filtering out much of the low frequency content of the signal.

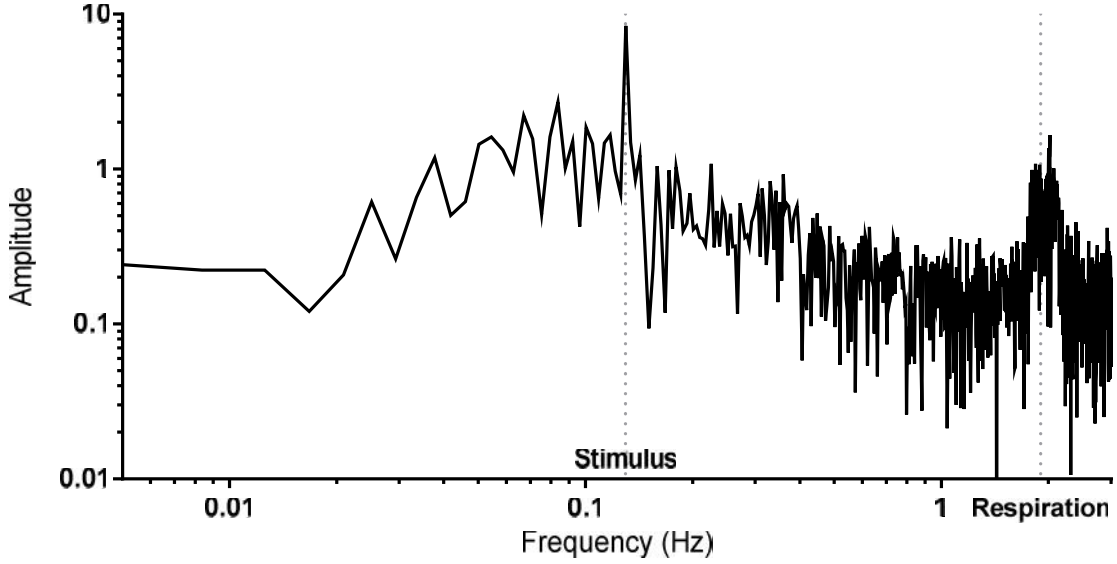

Figure 3.3 Amplitude spectrum of pixel data shown in figure 3.2. The stimulus frequency of 0.1296Hz is indicated, as well as the respiratory artifacts seen just below 2Hz. The stimulus response clearly stands out from the background activity.

A normal recording session of an animal last for 240 seconds, resulting in a total of 240s x 30frames/s = 7200 frames. Each frame consist of x by y pixels, and each pixel position is treated as a separate time series of 7200 values. So each of these x times y time series are processed as shown in figure 3.2 and 3.3, before an amplitude image is generated by taking the FFT amplitude at the stimulus frequency for each pixel location. However, because of uneven illumination and other factors, the relative change in the recorded signal at each location is more useful. This is calculated by dividing the amplitude of the signal by the average of the whole time series in the same pixel location. This calculated relative change is then used as the final representation of activity. Examples of two such amplitude images are shown in fig 3.4A and C.

In addition to the amplitude of the signal, the Fourier transform also provide information on the phase shift of the signal. The phase shift tells us how much the signal is delayed in

relation to the beginning of the recording, allowing us to relate the stimulus state to an area of cortex. Examples of such phase maps are shown in figure 3.4B and D. The phase angle in these maps describes the phase of the visual stimuli, with 0º signifying the middle of a stimulus cycle, 180º the start and -180º the end.

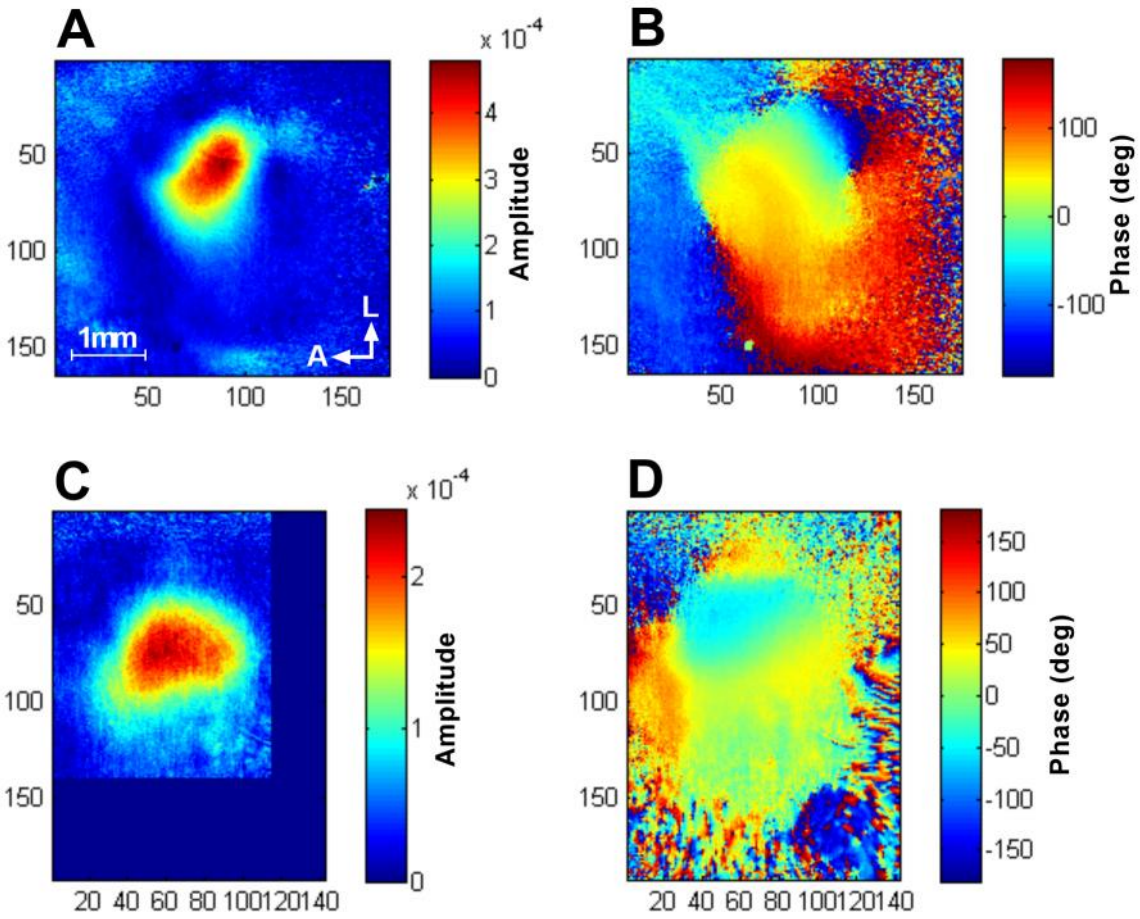

Figure 3.4 Example amplitude and phase images. (A) The response to a horizontal bar, spanning 20º, moving vertically across the stimulus monitor, (B) the corresponding phase response. (C) The response to a vertical bar moving horizontally across the monitor with the corresponding phase shown in (D). Notice the approximate 90º difference in the direction of the phase change in (B) versus (D).

The phase map in figure 3.4B is generated using a horizontal bar moving vertically, and a phase shift of +180º represents the top of the screen while -180º represents the very bottom. Figure 3.4D shows a phase map generated by a vertical bar moving horizontally, and compared 3.4C the phase shift do seem to be at about a 90º angle, as would be expected given the retinotopic mapping of visual cortex.

These phase maps do not take into account the hemodynamic delay, meaning these maps only indicate relative, not absolute phase, the maps are shifted by an unknown amount. This can be

corrected by presenting the visual stimulus in both directions, and generating maps for both of these directions. Subtracting the phase map generated by stimuli in one direction from the map generated by stimulus in the opposite direction will cancel the hemodynamic delay, and a true, absolute phase map is the result.

The best-case scenario would be that subsequent recordings from the same animal gives about equal response strength as well as phase maps, but this is often not the case. As shown in figure 3.5 subsequent recordings often result in quite variable amplitude maps. This variability was the one thing I ended up spending the most time investigating and trying to reduce. After having eliminated most other sources, I am convinced that the residual variance is caused by varying levels of biological background activity. It is known from researchers in the field that such variable measures are quite common (M.P. Stryker, personal communication).

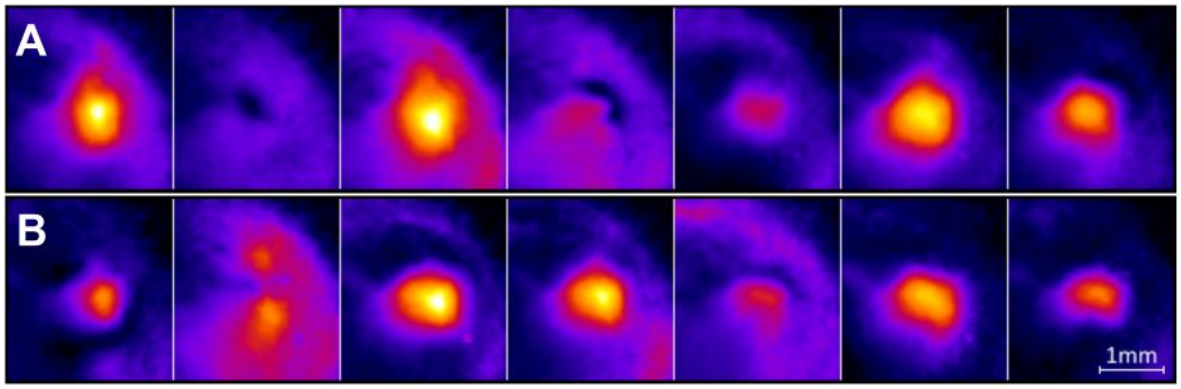

Figure 3.5 Series of recordings illustrating the variability of the recorded signal. (A) Recordings of contralateral eye response. (B) Recordings of ipsilateral eye response. All recordings are made in one recording session, each recording is 4 minutes long.

To get reliable and reproducible results I decided on two criteria for deciding if a recording was good enough to be included in the subsequent analysis. First, the amplitude map should show a sharply delineated area of activity, not bleeding out across large parts of the recorded area. Secondly, there should be at least some phase shift visible in the phase map. Recordings dominated by background activity will show a more or less constant phase across the whole map due to the synchronous activity, and this is an indication the recording is of low quality.

Amplitude maps are created for each eye separately by blocking one eye and recording the response through the unblocked eye. Several maps are averaged together, creating one map for the ipsilateral eye and one for the contralateral eye. Based on the maps an ODI can be

calculated for the animal (described in chapter 2.7), as shown in figure 3.6. The maps for the individual eyes are shown in 3.6A1 and 3.6A2, while the ODI for each individual pixel is shown in 3.6A3. 3.6C shows the distribution of ODI values in 3.6A3.

Figure 3.6B and D shows the same data after 3 days of MD, and the change in OD is clearly visible, with the distribution in 3.6D shifted towards the ipsilateral eye (more negative ODI).

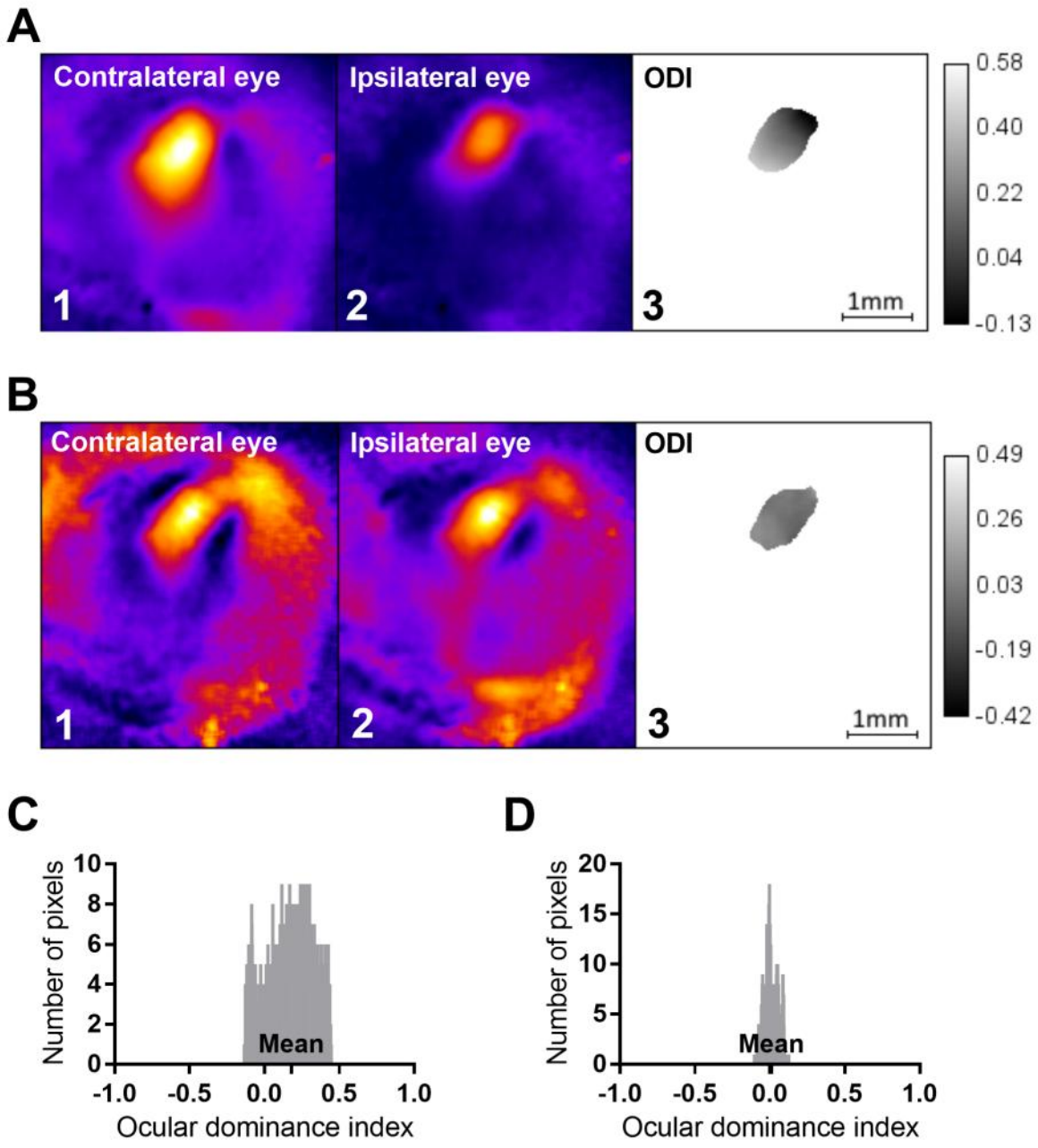

Figure 3.6 Example of shift in ocular dominance after MD. (A) Response strength before MD, contralateral eye (A1), ipsilateral eye (A2) and (A3) shows the ODI for each pixel of the responsive area. Note the stronger response from stimulation of the contralateral eye. (B) The ODI distribution of all the pixels in the responsive

area, with a mean of approximately 0.2. (C) Recording after 3 days of MD (same setup as in A), while (D) shows the ODI distribution, with a mean close to zero.

3.2 Aggrecan knockout

After having verified the OIIS setup, it was utilized to investigate the effect on OD plasticity of adult mice after knocking out aggrecan in their primary visual cortices.

3.2.1 Histology

Histology was performed to verify the accuracy and effectiveness of the viral injections, as well as to investigate the effects on aggrecan and PNN expression.

In order to test whether the transgenic animals had normal expression of PNNs before the expression of aggrecan was knocked out, we labeled sections from the untreated hemisphere of animals homozygous with the floxed *ACAN* genes with WFA and compared them to WFA labeled sections from wild type animals. The untreated cortical area of transgenic animals should express aggrecan at the same level as the wild-type animals and the level of PNN expression should also be comparable. Visual inspection of the labeled sections, shown in figure 3.7, revealed no differences in the structure or the amount of PNNs (Figure 3.7).

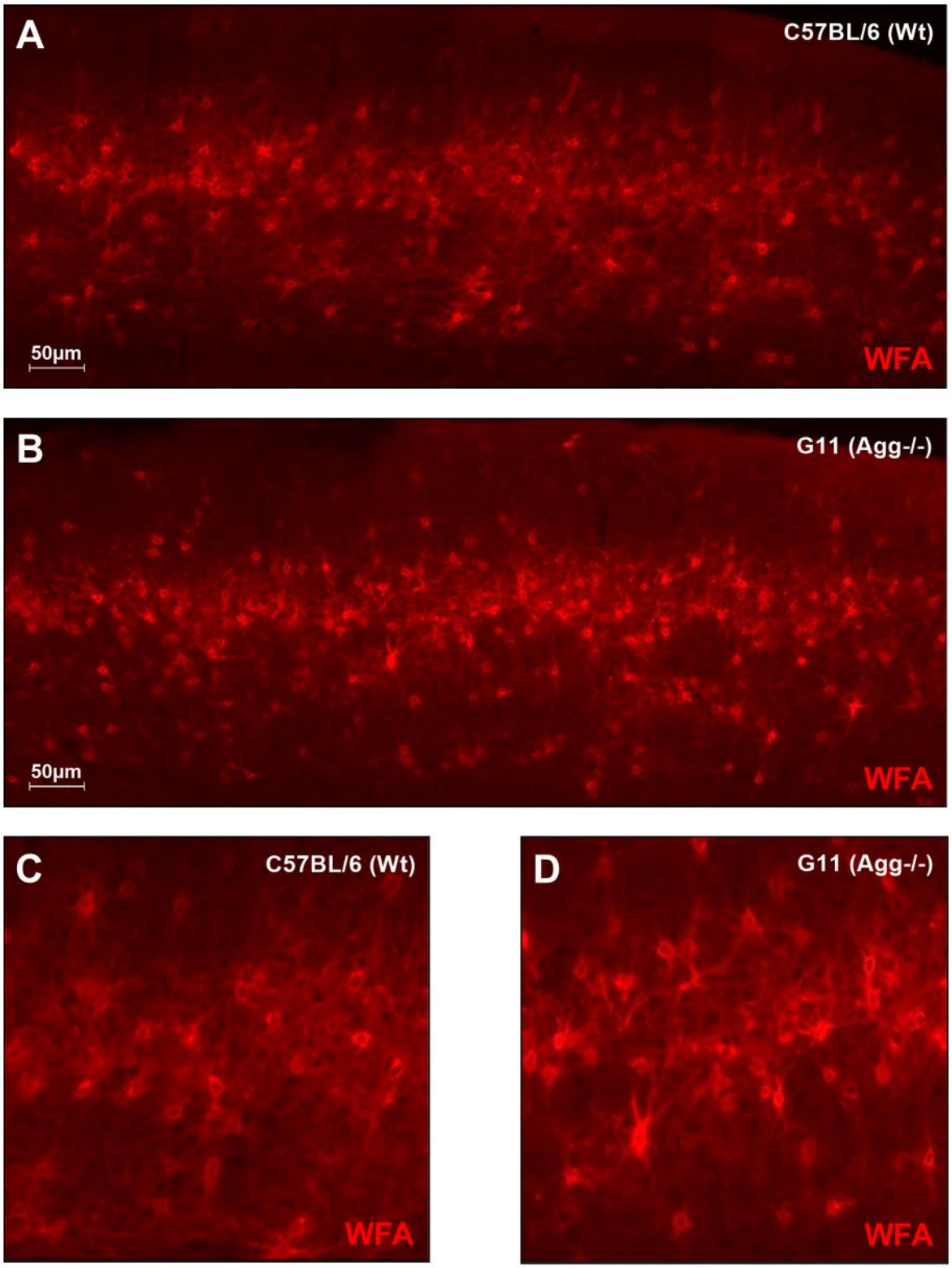

Figure 3.7 Mice homozygous for the floxed *ACAN* gene have similar expression of PNNs as wild type C57BL/6 mice. WFA labeled sections from wild type C57BL/6 (A) and untreated hemisphere of of the transgenic (B) mice. (C) and (D) shows magnified sections of (A) and (B). No differences in the amount or pattern of labeling are visible.

We also investigated the relationship between aggrecan expression and PNN expression, and as shown in figure 3.8 the degree of colocalization was found to be close to 100%. This result is in accordance with previous findings that aggrecan is an important part of the PNNs, as described in chapter 1.1 and 1.2.

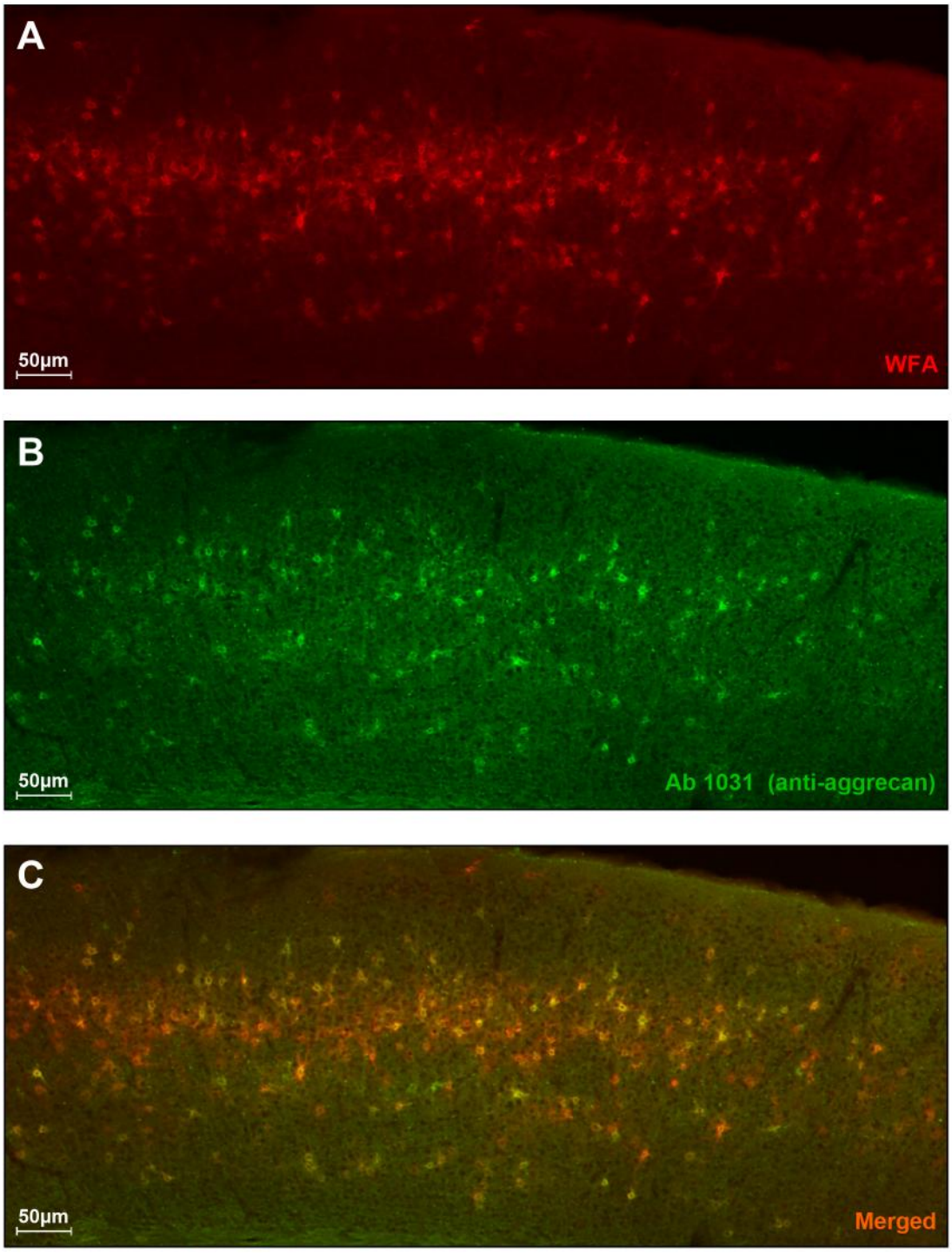

Figure 3.8 Complete overlap between aggrecan and WFA. WFA labeled section (A) and Ab 1031, an anti aggrecan label, labeled section (B). (C) A merge of A and B, showing the overlap between the two labels, which is close to 100%. The sections are from a transgenic mouse homozygous for the floxed *ACAN* gene.

Having verified that aggrecan expression do overlap with PNNs, histology was performed on treated transgenic animals.

The injected virus cause expression of GFP, in addition to Cre, and a dual labeling was performed for GFP as well as PNNs. The GFP labeling allowed us to verify the strength and location of the viral infection, while WFA labeling allowed us to determine the level of PNN expression.

The result of this double labeling is shown in figure 3.9. 3.9A shows the GFP labeling, showing the extent of the viral infection in the area of V1, indicating that the virus has spread throughout most of V1. 3.9B shows the WFA labeling, and compared to the WFA labeling in figure 3.8 the level of PNN expression is clearly reduced in the area of viral infection. The area of reduced PNN expression in figure 3.9B co-localize completely with the area of GFP expression in 3.9A, a merge of the two images is shown in figure 3.9C.

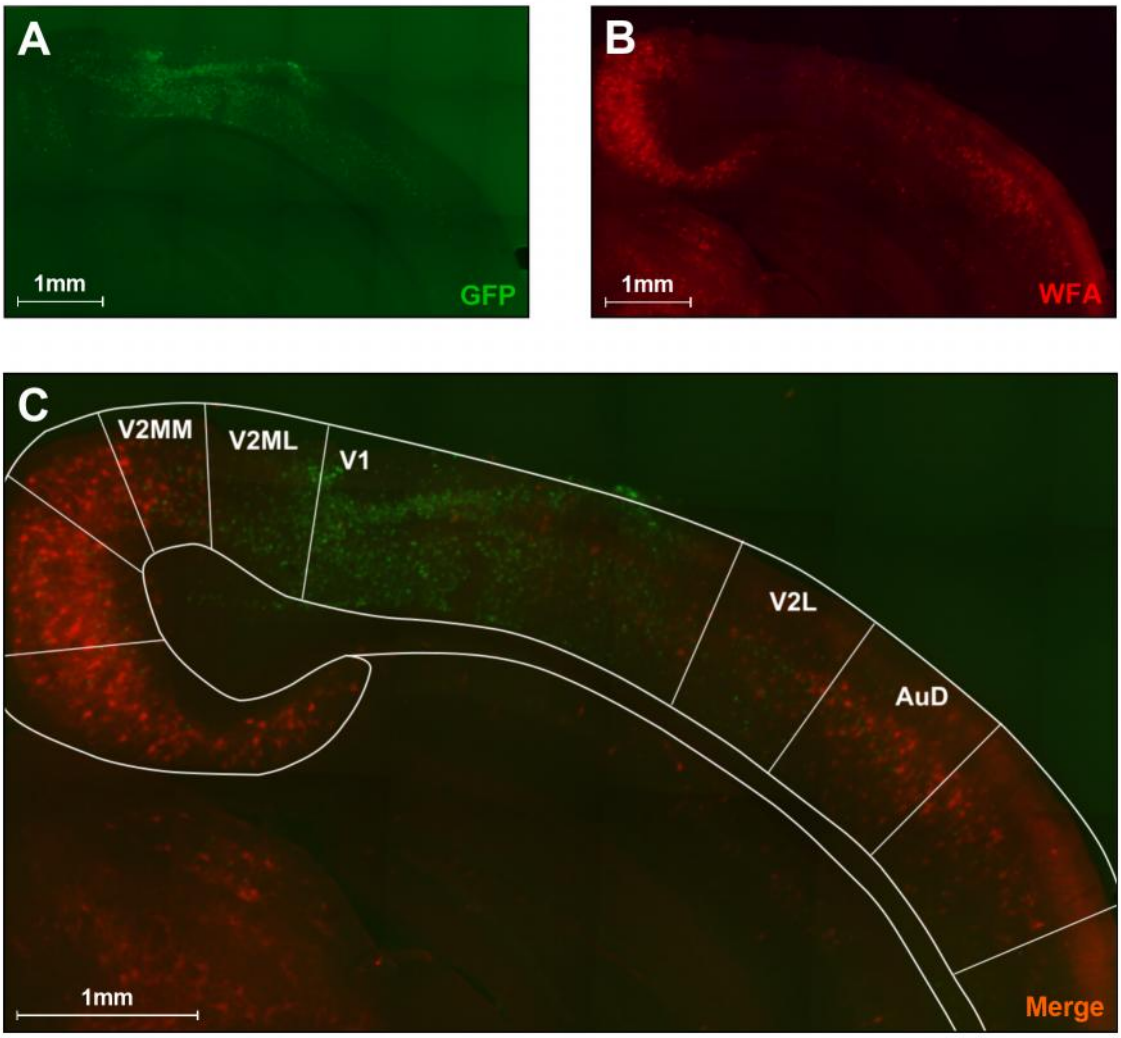

Figure 3.9 Viral injection. (A) Virus infected cells labeled with GFP. (B) WFA labeling of PNNs. (C) A merge between (A) and (B), clearly showing how the areas infected by the virus show much reduced levels of WFA labeling, an indicator of reduced levels of PNNs. An overlay indicating cortical areas is also included. (Sections are from mouse #0201) (V2MM and V2ML = mediomedial and lateromedial secondary visual cortex, V1 = primary visual cortex, V2L = lateral secondary visual cortex, AuD = primary auditory cortex)

Having verified that the virus injection was in the right place, and that it resulted in a strong reduction of WFA labeling, an indicator of reduced PNN expressions, the next step was to investigate whether knocking down aggrecan also affected ocular dominance plasticity of adult mice. This was done conducting repeated measures of visual cortical activity using OIIS.

3.2.2 Ocular dominance plasticity

The ocular dominance plasticity of the treated animals was characterized using OIIS. The whole protocol, as described in chapter 2.7, was successfully carried out on five treated animals. For three animals, recordings were not completed due to technical problems.

Recordings were carried out in accordance with the timeline shown in figure 2.2. Results are shown in figure 3.10.

Figure 3.10A shows the ODI of each individual animal at the different time points. With the exception of animal #0207, which shows a somewhat abnormal pre-MD value, all animals show an ODI that shifts towards the ipsilateral eye after 3 days of MD, and a shift back towards the contralateral eye after 2 days of recovery.

Figure 3.10B shows the ODI shift compared to the pre-MD value. Again, the negative ODI shift of the post-MD time point becomes visible, as well as the recovery back towards the pre-MD values.

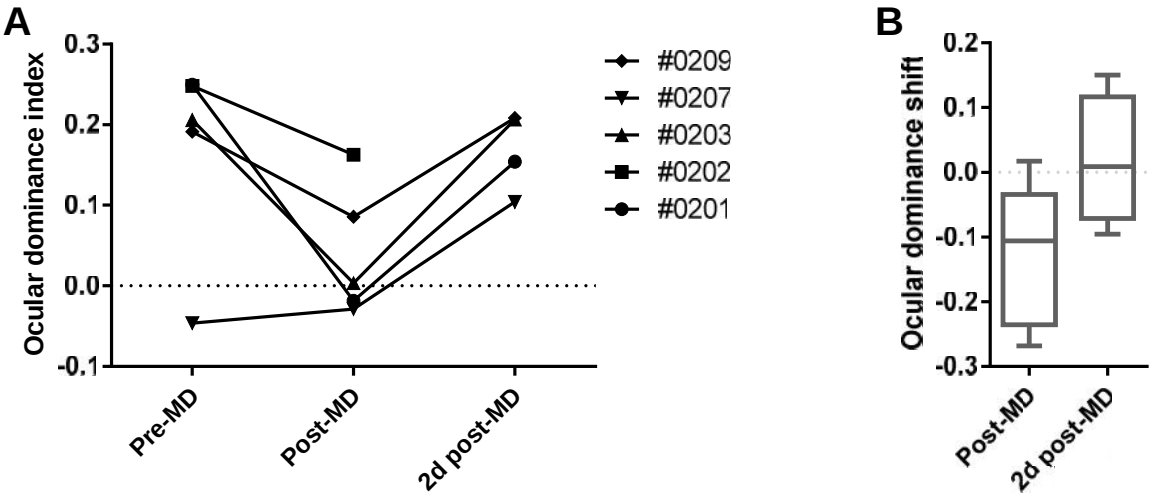

Figure 3.10 Mice with local knockout of aggrecan in visual cortex show high levels of plasticity during MD. (A) Ocular dominance index of the individual animals at the three different time points. The difference in response between the pre-MD and post-MD group was not found to be significant using Wilcoxon matched pairs test ($p = 0.1250$). (B) The ocular dominance shift relative to the pre-MD group.

After the first three animals a change was introduced to the visual stimuli used during recordings, the stimuli was changed to a faster moving bar. This was done to improve the SNR of the recordings. However, as figure 3.11 shows there was no significant difference in the response strength to the two types of stimuli. Thus, the recorded responses between animals are comparable.

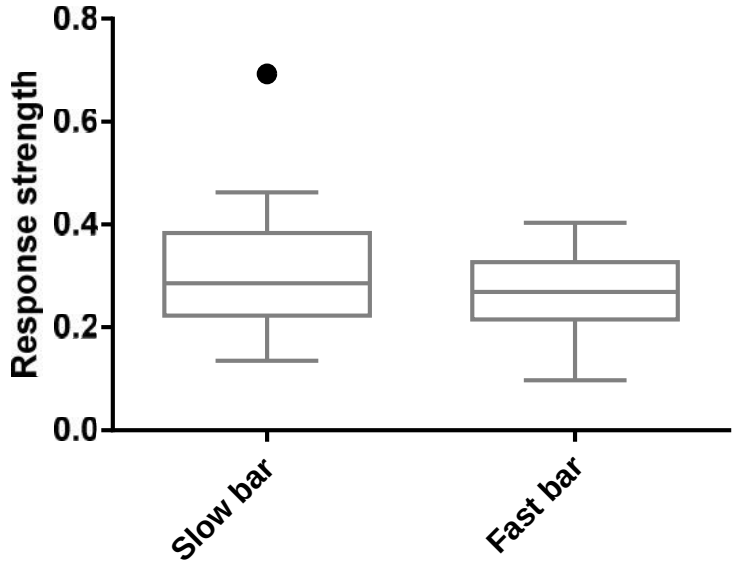

Figure 3.11 Averaged response to slow vs fast visual stimuli. The response to the slow bar (n = 50) is not significantly different from the response to the fast bar (n = 30, p = 0.345). Data was analyzed using an unpaired, two-tailed Mann-Whitney test.

4 Discussion

In my thesis, I setup and verified OIIS as a method to quantify ocular dominance plasticity. Furthermore, using the first characterization of a newly developed conditional knockout mouse of the aggrecan gene in CNS, I provided data confirming that aggrecan has a central role in the PNNs *in-vivo*. Finally, using OIIS in combination with viral vectors I induced local knockout of aggrecan in visual cortex and show that removal of aggrecan in the adult brain increase the level of OD plasticity to levels similar to what is found in juvenile mice during the critical period.

4.1 Methodological considerations

The OIIS is very well suited to do this kind of ocular dominance plasticity study (Cang et al., 2005). The amount of time needed up front for preparing the animals is quite short, especially when doing the imaging transcranially. It also makes it possible to follow OD changes in an animal over time, which enable powerful within-animal comparisons. However, as the method does not directly measures neural activity, only changes to blood circulation, the results are easily confounded by other sources of circulatory changes and this has to be taken into consideration when analyzing the results. The amount of time needed for a full recording session should also be taken into consideration. The use of OIIS in combination with periodic stimulus and FFT to extract the response cuts the time needed by a factor of 10 to 100 compared to OIIS using episodic stimuli as well as electrophysiological methods (Kalatsky and Stryker, 2002).

An alternative method for OD characterization would be electrophysiological recordings. This does involve a more complex preparation, necessitating a craniotomy to gain access to the tissue. Craniotomy increases the chance of damaging the cortex and increases the risk of infection. On the other hand, electrophysiology is a direct measure of the neural activity with less risk of the results being confounded by other factors.

One critical factor when doing OD characterization after MD involves the opening of the sutured eye during the post-MD recording. If the eye is not fully open during this recording session, which is a risk given that the eyelids tends to close just after opening, the result would be the same as if an actual ODI shift had taken place. However, special precautions

were taken during the post-MD recordings to prevent this, with the openness of the eye being checked, and adjusted if necessary, several times during the recording session.

The use of the Cre-lox system to do a conditional knockout of aggrecan is a crucial part of this study. As mentioned earlier constitutive aggrecan knockout mice will not survive birth, making it impossible to do this kind of functional studies. The Cre-lox system, combining a transgenic mouse line with viral vectors for restriction of the gene perturbation is a leap forward for investigating molecular mechanisms of neural function.

4.2 Setting up OIIS

A large part of the project consisted of setting up OIIS, and even though most of the challenges encountered was solved in a more or less satisfactory way, I still think there are room for improvements, both to the technical solutions and with regard to the recording protocol.

There are still challenges related to providing even illumination of the skull, while at the same time preventing the formation of highlights. One way to improve this would be by placing some sort of light diffuser over the LEDs, this would reduce the amount of specular reflections greatly. Another technique that I did try, with some success, was to apply silicone oil on top of the skull during the recording, this did indeed reduce the amount of specular highlights. But this technique do entail some way to keep the oil contained in the right place, and the oil would probably lead to contaminants accumulating between sessions if not cleaned up properly. The possibility of adjusting the intensity of the individual LEDs would also help. This was done to a certain extent by inserting a piece of paper in front of one of the LEDs, but this proved very sensitive to mechanical disturbances.

The choice of lenses, 2×50mm giving a magnification of 1×, was initially done with a different camera in mind. The change of camera resulted in a FOV of 12×12mm, which is quite big for imaging V1, being only about 2×3mm in mice. Exchanging one of the lenses with a 135mm would increase the magnification of the setup to 135mm/50mm = 2.7×, allowing for much more detailed maps.

The acquisition software could also be improved in several ways, allowing less complicated use as well as a potential increase in quality. In the current setup, the stimulus synchronization

server is implemented as a standalone application, but it would simplify things if it were implemented as part of the image acquisition software. This would lead to one less piece of software to remember to start, as well as making the actual timing information easier to calculate.

Another improvement that could potentially improve the quality of recordings is the addition of a real-time FFT view in the acquisition software. It would make it much easier to determine the state of the animal, and decide whether it is stable enough to start recording. With the current setup, a complete recording of at least 120 seconds must be completed and then analyzed before the results are available, making adjustments to the level of anesthesia difficult.

The large variability in the recorded response shown in figure 3.6 seem to me to stem from changing levels of vasomotion, and this seem to depend in a large part on the level of anesthesia. It is well known from the literature that the level of anesthesia are important for visual responses and the hemodynamic response in general (Constantinides et al., 2011). This is consistent with my findings that higher concentrations of isoflurane resulted in weaker stimulus responses, but also less background activity. Using concentrations used in other studies, around 0.6-0.9% isoflurane (Davis et al., 2015; Fu et al., 2015) proved too low, with animals starting to wake up during the recording session. In most cases I had to use a minimum of 0.9% to keep animals quite, and I often had to use concentrations as high as 1.1 to 1.2%. The reason for this discrepancy is unknown, but it could be caused the use of different equipment for delivery of the gas as well as differences in the design of custom-made masks for gas delivery. Another factor is the fact that isoflurane is administered in combination with chlorprothixene, and the time taken from injection to the start of recording could have an effect.

For the OD characterization of the aggrecan knockouts, we decided to do the imaging transcranially, covering the exposed skull with liquid bandage to prevent the bone from becoming opaque. This is less invasive and time-efficient, compared to doing a craniotomy, which has been a common procedure for OIIS in adult animals before (Fu et al., 2015). A compromise could be a thinned skull approach, were the skull is thinned before application of the liquid bandage (Yang et al., 2010). This would probably increase the signal-to-noise ratio and result in better quality of the generated maps with a moderate increase in the work done on each animal. Whether such an increase in map quality is really needed for OD plasticity

assays is another question, but for the generation of retinotopic maps it could be worth the effort.

4.3 Aggrecans role in plasticity

The histology confirmed that the PNNs overlap more or less perfectly with aggrecan, which is in accordance with what is known about aggrecan being a known component of the PNNs. It also confirmed the injection site in V1, along with a viral infection that encompassed all of V1. Figure 3.10 clearly shows how the areas infected by the virus exhibits a strong reduction in PNN expression. This does imply that aggrecan is indeed a critical component of the PNNs, and that the PNNs disappear in its absence, these findings are in line with findings of at least one earlier study (Giamanco et al., 2010).

Getting the OIIS setup up and running took longer than expected, and this limited the time available to carry out the OD plasticity experiments. I therefore prioritized to test the injected animals at the cost of control animals in the study. In order to secure successful MDs I also reduced the MD period from the normally used 4 days to 3 days.

Untreated transgenic animals will be used as a control group. This will allow us to eliminate the possibility that the genetic changes itself are responsible for the observed increase in plasticity. Another control group to be included will be a sham-operated group of transgenic animals eliminating any effect of the physical injection. However, given the large amount of time that passed between injection of the virus and recording it is unlikely this affected the results. A group of wild type animals injected with the virus can be tested, to eliminate the chance that any increase in plasticity is a result of the viral infection itself, and not from knocking out aggrecan.

With the lack of control animals, I cannot rule out effects of the recording protocol and subsequent treatment of the animals as a source of the observed OD shift.

The choice to reduce the MD period from four to three days was taken to reduce the chance that eyelid sutures would come undone, head bars falling off and the skull becoming too opaque for imaging, complications I could not afford due to time-constraints. Even though most studies employ MD periods of four days or longer, earlier studies have shown ODI shifts after three days of MD (Kaneko et al., 2010; Sternberg and Hamilton, 1981), and at least one

study have shown ODI shifts after as little as 1-2 days of MD in juvenile mice (Sato and Stryker, 2008).

Even if adult mice also have been reported to possess a certain degree of OD plasticity (Sternberg and Hamilton, 1981), the ODI shift after 3 days of MD is much smaller than what I have found for these animals. The results in figure 3.10 are therefore not explainable as normal adult levels of OD plasticity for wild type C57BL/6 mice, indicating that we are indeed looking at an increased level of plasticity.

The level of OD plasticity shown in figure 3.10, if adjusted for 3 days of MD instead of 4 days, is comparable to previous studies on critical period animals (Cang et al., 2005) and larger than what has been found in adult animals (Sato and Stryker, 2008). This supports that the shift in OD plasticity in the current experiment is due to genetic removal of aggrecan.

We cannot rule out that aggrecan is involved in some other unknown process regulating plasticity. However, aggrecan is an important constituent of the PNNs and knocking it out results in strongly reduced expression of PNNs, as shown in figure 3.9, combined with an increased level of ocular dominance plasticity, indicated by figure 3.10. These findings support the hypothesis that the PNNs are involved in regulating neuronal plasticity.

4.4 Future perspectives

The results of this study need to be complemented by further work including proper controls. This will strengthen the findings by eliminating sources of error.

Although there were no indications of distorted retinotopic maps after aggrecan KO, a detailed characterization of retinotopic maps of mice both before and after aggrecan KO will be important to investigate whether the KO affects the maps. Earlier studies where the PNNs have been removed have not found any effects on the retinotopic maps, but verifying this for the aggrecan KO will shed light in the role of PNNs for normal maps in the cortex.

One could also compare the plasticity of both treated and untreated juvenile transgenic animals to adult transgenic animals. Treating animals before the closure of the critical period should also result in animals that retain a heightened level of plasticity for the rest of their life.

Understanding neuroplasticity, and being able to control it, could have important consequences in several areas of human life. It could allow us to cure amblyopia and allow patients paralyzed by spinal cord injuries to walk again.

5 References

Bliss, T.V., Lømo, T., 1973. Long lasting potentiation of synaptic transmission in the dentate area of the anaesthetized rabbit following stimulation of the perforant path. The Journal of Physiology 232, 331–356.

Brainard, DH, 1997. The psychophysics toolbox. Spatial vision.

Cang, J., Kalatsky, V.A., Löwel, S., Stryker, M.P., 2005. Optical imaging of the intrinsic signal as a measure of cortical plasticity in the mouse. Visual Neuroscience.

Carulli, D., Pizzorusso, T., Kwok, J., Putignano, E., Poli, A., Forostyak, S., Andrews, M., Deepa, S., Glant, T., Fawcett, J., 2010. Animals lacking link protein have attenuated perineuronal nets and persistent plasticity. Brain 133, 2331–47.

Carulli, D., Rhodes, K.E., Brown, D.J., Bonnert, T.P., Pollack, S.J., Oliver, K., Strata, P., Fawcett, J.W., 2006. Composition of perineuronal nets in the adult rat cerebellum and the cellular origin of their components. The Journal of Comparative Neurology 494, 559–77.

Constantinides, C., Mean, R., Janssen, B.J., 2011. Effects of isoflurane anesthesia on the cardiovascular function of the C57BL/6 mouse. ILAR Journal / National Research Council, Institute of Laboratory Animal Resources 52, e21–31.

Davis, M., Velez, D., Guevarra, R., Yang, M., Habeeb, M., Carathedathu, M., Gandhi, S., 2015. Inhibitory Neuron Transplantation into Adult Visual Cortex Creates a New Critical Period that Rescues Impaired Vision. Neuron.

Deepa, S.S., Carulli, D., Galtrey, C., Rhodes, K., Fukuda, J., Mikami, T., Sugahara, K., Fawcett, J.W., 2006. Composition of perineuronal net extracellular matrix in rat brain: a different disaccharide composition for the net-associated proteoglycans. The Journal of Biological Chemistry 281, 17789–800.

Frischknecht, R, Heine, M, Perrais, D, 2009. Brain extracellular matrix affects AMPA receptor lateral mobility and short-term synaptic plasticity. Nature Neuroscience.

Fu, Y., Kaneko, M., Tang, Y., Alvarez-Buylla, A., Stryker, M., 2015. A cortical disinhibitory circuit for enhancing adult plasticity. eLife.

Garcia, E., Mills, A., 2002. Getting around lethality with inducible Cre-mediated excision. Seminars in Cell & Developmental Biology 13, 151158.

Giamanco, KA, Morawski, M, Matthews, RT, 2010. Perineuronal net formation and structure in aggrecan knockout mice. Neuroscience.

Giamanco, K.A., Matthews, R.T., 2012. Deconstructing the perineuronal net: cellular contributions and molecular composition of the neuronal extracellular matrix. Neuroscience 218, 367–84.

Gordon, JA, Stryker, MP, 1996. Experience-dependent plasticity of binocular responses in the primary visual cortex of the mouse. The Journal of Neuroscience.

Grinvald, A., Lieke, E., Frostig, R.D., Gilbert, C.D., Wiesel, T.N., 1986. Functional architecture of cortex revealed by optical imaging of intrinsic signals. Nature.

Hentschke, H., Schwarz, C., Antkowiak, B., 2005. Neocortex is the major target of sedative concentrations of volatile anaesthetics: strong depression of firing rates and increase of GABAA receptor mediated inhibition. European Journal of Neuroscience 21, 93–102.

Hubel, D.H., Wiesel, T.N., 1970. The period of susceptibility to the physiological effects of unilateral eye closure in kittens. The Journal of Physiology 206, 419–436.

Hughes, J.R., 1958. Post-tetanic potentiation. Physiological reviews 38, 91–113.

Jacobs, G.H., Williams, G.A., Fenwick, J.A., 2004. Influence of cone pigment coexpression on spectral sensitivity and color vision in the mouse. Vision Research 44, 1615–1622.

Kalatsky, V., Stryker, M., 2002. New Paradigm for Optical Imaging: Temporally Encoded Maps of Intrinsic Signal. Neuron 38.

Kaneko, M., Cheetham, C.E., Lee, Y.-S., Silva, A.J., Stryker, M.P., Fox, K., 2010. Constitutively active H-ras accelerates multiple forms of plasticity in developing visual cortex. Proceedings of the National Academy of Sciences 107, 19026–19031.

Kaspar, B.K., Vissel, B., Bengoechea, T., Crone, S., Randolph-Moore, L., Muller, R., Brandon, E.P., Schaffer, D., Verma, I.M., Lee, K.-F.F., Heinemann, S.F., Gage, F.H., 2002. Adeno-associated virus effectively mediates conditional gene modification in the brain. Proceedings of the National Academy of Sciences 99, 2320–5.

Matthews, RT, Kelly, GM, Zerillo, CA, 2002. Aggrecan glycoforms contribute to the molecular heterogeneity of perineuronal nets. The Journal of Neuroscience.

McRae, P.A., Rocco, M.M., Kelly, G., Brumberg, J.C., Matthews, R.T., 2007. Sensory deprivation alters aggrecan and perineuronal net expression in the mouse barrel cortex. The Journal of Neuroscience 27, 5405–5413.

Merzenich, M.M., Nelson, R.J., Stryker, M.P., Cynader, M.S., Schoppmann, A., Zook, J.M., 1984. Somatosensory cortical map changes following digit amputation in adult monkeys. The Journal of Comparative Neurology 224, 591–605.

Morawski, Brückner, Arendt, Matthews, 2012. Aggrecan: Beyond cartilage and into the brain. The International Journal of Biochemistry & Cell Biology.

Pizzorusso, T., Medini, P., Berardi, N., Chierzi, S., Fawcett, J., Maffei, L., 2002. Reactivation of Ocular Dominance Plasticity in the Adult Visual Cortex. Science 298, 1248–1251.

Pizzorusso, T., Medini, P., Landi, S., Baldini, S., Berardi, N., Maffei, L., 2006. Structural and functional recovery from early monocular deprivation in adult rats. Proceedings of the National Academy of Sciences 103, 8517–8522.

Ratzlaff, E.H., Grinvald, A., 1991. A tandem-lens epifluorescence macroscope: hundred-fold brightness advantage for wide-field imaging. Journal of Neuroscience methods 36, 127–137.

Rauch, U., Hirakawa, S., Oohashi, T., Kappler, J., Roos, G., 2004. Cartilage link protein interacts with neurocan, which shows hyaluronan binding characteristics different from CD44 and TSG-6. Matrix Biol. 22, 629–39.

Rittenhouse, E., Dunn, L.C., Cookingham, J., Calo, C., Spiegelman, M., Dooher, G.B., Bennett, D., 1978. Cartilage matrix deficiency (cmd): a new autosomal recessive lethal mutation in the mouse. Journal of Embryology and Experimental Morphology 43, 71–84.

Sadato, N., Pascual-Leone, A., Grafman, J., Ibañez, V., Deiber, M.P., Dold, G., Hallett, M., 1996. Activation of the primary visual cortex by Braille reading in blind subjects. Nature 380, 526–8.

Sato, M., Stryker, M., 2008. Distinctive Features of Adult Ocular Dominance Plasticity. Journal of Neuroscience 28, 10278–10286.

Sauer, B., Henderson, N., 1988. Site-specific DNA recombination in mammalian cells by the Cre recombinase of bacteriophage P1. Proceedings of the National Academy of Sciences 85, 5166–5170.

Sternberg, N., Hamilton, D., 1981. Bacteriophage P1 site-specific recombination. I. Recombination between loxP sites. Journal of Molecular Biology 150, 467–86.

Thaler, L., Arnott, S.R., Goodale, M.A., 2011. Neural correlates of natural human echolocation in early and late blind echolocation experts. PLoS ONE 6, e20162.

Wang, D., Fawcett, J., 2012. The perineuronal net and the control of CNS plasticity. Cell and Tissue Research 349, 147–60.

Wiesel, T.N., Hubel, D.H., 1963. Single-Cell Responses In Striate Cortex Of Kittens Deprived Of Vision In One Eye. Journal of Neurophysiology 26, 1003–17.

Wiesel, T.N., Hubel, D.H., 1965. Extent of recovery from the effects of visual deprivation in kittens. Journal of Neurophysiology 28, 1060–1072.

Yang, G., Pan, F., Parkhurst, C.N., Grutzendler, J., Gan, W.-B., 2010. Thinned-skull cranial window technique for long-term imaging of the cortex in live mice. Nature protocols 5, 201–208.

6 Appendix

6.1 List of abbreviations

AAV	Adeno associated virus
AOI	Area of interest
CCD	Charge coupled device
chABC	Chondriotinase ABC
CNS	Central nervous system
CP	Critical period
CSPG	Chondroitin sulphate proteoglycan
ECM	Extra cellular matrix
fMRI	Functional magnetic resonance imaging
GFP	Green fluorescent protein
IP	Intraperitoneal
KO	Knock-out
LED	Light emitting diode
MD	Monocular deprivation
OD	Ocular dominance
ODI	Ocular dominance index
OIIS	Optical imaging of intrinsic signals
PNN	Perineuronal net
SC	Subcutaneous
SNR	Signal to noise ratio
V1	Primary visual cortex
WFA	Wisteria floribunda agglutinin